DOI 10.1515/mgmc-2013-0051 — Main Group Met. Chem. 2014; 37(1-2): 11–24

Gabriele Kociok-Köhn, Mary F. Mahon*, Kieran C. Molloy* and Anna L. Sudlow

Synthesis and structures of Cu-Cl-M adducts (M=Zn, Sn, Sb)

Abstract: The novel bimetallic adducts $[(Ph_3P)_2CuCl]_2.ZnCl_2$ (**1**), $\{[(Me_3P)CuCl]_2.ZnCl_2\}_n$ (**2**), $[(Me_3P)_4Cu]^+[(Me_3P)_2Cu(Cl)_2ZnCl_2]^-$ (**3**), $(Ph_3P)_2CuCl.SnCl_2$ (**4**), $(Me_3P)_3CuSnCl_3$ (**5**), $[(Ph_3P)_2CuCl.SbCl_3]_2$ (**6**) and $(Ph_3P)_3CuCl.SbCl_3$ (**7**) have been synthesized from combinations of R_3P, CuCl and one of $ZnCl_2$, $SnCl_2$ or $SbCl_3$, and their structures were determined. $[(Me_3P)_2Cu]^+[HPMe_3]_2^+[Sb_2Cl_9]^{3-}$ (**8**) and $[(Me_3P)_4Cu]^+[(Me_3P)_2Sb_2Cl_7]^-$ (**9**) have been isolated as minor by-products from the reaction of Me_3P, CuCl and $SbCl_3$, and their structures were also determined.

Keywords: antimony; bimetallic; chloride; copper; tin; X-ray crystallography; zinc.

***Corresponding authors: Mary F. Mahon,** (for crystallographic correspondence), Department of Chemistry, University of Bath, Claverton Down, Bath BA2 7AY, UK, e-mail: m.f.mahon@bath.ac.uk; and **Kieran C. Molloy,** (for general correspondence), Department of Chemistry, University of Bath, Claverton Down, Bath BA2 7AY, UK, e-mail: k.c.molloy@bath.ac.uk,
Gabriele Kociok-Köhn and Anna L. Sudlow: Department of Chemistry, University of Bath, Claverton Down, Bath BA2 7AY, UK

Introduction

We have an ongoing interest in the chemistry of precursors for ternary and quaternary multimetal chalcogenides such as Cu_2SnE_3, $CuSbE_2$ and Cu_2ZnSnE_4 (E=S, Se), which are currently being actively studied as novel energy materials incorporating low-cost, earth-abundant metals (Kociok-Köhn et al., 2013). For example, Cu_2ZnSnS_4 (CZTS) or the related $Cu_2ZnSnSe_4$ (CZTSe) has been used as an absorber layer in photovoltaic cells with efficiencies that have now exceeded 11% (Abermann, 2013; Colombara et al., 2013). $CuSbS_2$ is, like the widely exploited $CuInS_2$, part of the I-III-VI_2 class of semiconductors with a chalcopyrite structure. $CuSbS_2$ is a direct semiconductor with a band gap of 1.5 eV and as such is an ideal candidate for use as a solar absorber layer in a thin-film solar cell (Lazcano et al., 2001; Dufton et al., 2012; Temple et al., 2012), while the price of antimony is considerably lower than that of indium (Manolache et al., 2007). However, unlike CZTS/Se, this absorber layer is not, as yet, very widely investigated (Nair et al., 2005; Manolache and Duta, 2007), and to our knowledge, no efficiencies for cells with $CuSbS_2$ absorber layers have been reported. Cu_2SnS_3 is an example of a ternary material with a high optical absorption coefficient (ca. 10^4 cm^{-1}) (Guan et al., 2013) and a band gap in the range 1.00–1.19 eV (Su et al., 2012; Guan et al., 2013; Wang et al., 2013) from which solar cells with efficiencies of ca. 2.5% have been fabricated (Chino et al., 2012; Koike et al., 2012). Cu_2SnS_3 has also been used as an intermediate in the synthesis of CZTS nanoparticles (Park et al., 2013).

One of the major challenges in the materials chemistry of these systems is the deposition of thin films from appropriate precursors, particularly in a dynamic methodology such as chemical vapor deposition (CVD), which allows for relatively rapid, large-scale coatings to be fabricated. The dominant problem is matching the decomposition profiles of two or three precursors such that the correct stoichiometry is achieved. Indeed, with regard to CZTS, although a number of routes to thin films *via* spray pyrolysis (Nakayama and Ito, 1996), sulfurization of electrodeposited metal precursors (Kurihara et al., 2009), non-vacuum electroplating (Ennaoui et al., 2009), spin coating (Yeh et al., 2009), pulsed laser deposition (Moriya et al., 2007) and photochemical deposition (Moriya et al., 2006), sputtering (Ito and Nakazawa, 1988) and co-evaporation (Tanaka et al., 2006) have been reported, there have only been two reports of a successful CVD route to this material (Ramasamy et al., 2012; Kociok-Köhn et al., 2013).

One way in which this problem could be mitigated is by the use of precursors that embody more than one metal in the correct relative ratio in a single precursor, e.g., Cu_2Zn, Cu_2Sn, CuSb, which would reduce the total number of precursors required in any deposition process. However, to our knowledge, relatively few systems of this type are known (e.g., Nayek et al., 2008), particularly when the need for simplicity (to offer the best chance of good volatility and/or solubility) is also considered. We have thus become interested in the synthesis of simple mixed-metal halide adducts that may provide an entry point into this area of chemistry. There are just three reported molecular structures involving the Cu-X-Sb (X=halogen) linkage, and all involve the $[SbF_6]^-$ anion (Gardberg and Ibers, 2001; Manson et al., 2009; Nakajima et al., 2011). The Cu-X-Sn

system is even rarer with only two cited examples (Veith et al., 1989; Han et al., 2009), and although there are 11 structures that incorporate the Cu-X-Zn moiety, all but two (Mandal et al., 1988; Nakamura et al., 2001) of these are based on coordinated $[ZnCl_4]^{2-}$ anions (Mandal et al., 1988; Zang et al., 1990; Gou et al., 1992; Prins et al., 1996; Gladkikh et al., 1997; Martin et al., 1998; Curtis and Gladkikh, 2000; Pryma et al., 2003; Shevchenko et al., 2005). Note that framework, rather than molecular, systems such as $[Cu_nZn_{m-n}Cl_{2m}]^{n-}$ are known (Martin et al., 1998). In the light of this, we now report the synthesis and structural characterization of novel molecular examples of each of these systems [Cu/Zn, Cu/Sn, Cu/Sb].

Results and discussion

Cu-Zn bimetallic systems

$[(Ph_3P)_2CuCl]_2.ZnCl_2$ (**1**) was synthesized following a literature method for the synthesis of $(Ph_3P)_2CuInCl_4$ (Margulieux et al., 2010) by direct reaction of $ZnCl_2$ and $(Ph_3P)_2CuCl$ in toluene. Although the initial synthesis involved reagents in a 1:1 stoichiometry, the resulting product always formulated as Cu_2Zn; as a result, the synthetic procedure was modified to improve the yield. Similarly, $\{[(Me_3P)CuCl]_2.ZnCl_2\}_n$ (**2**) and $[(Me_3P)_4Cu]^+[(Me_3P)_2Cu(Cl)_2ZnCl_2]^-$ (**3**) were synthesized using a similar route, from $ZnCl_2$, CuCl and Me_3P at 60°C in toluene without prior formation and isolation of $(Me_3P)_2CuCl$. Although **2** retains the 2Cu:Zn ratio seen in **1**, it contains less phosphine than expected; thus the reaction was repeated with a larger quantity of phosphine, which subsequently afforded the ionic species **3**, in which the P:Cu:Zn ratio reflects that of the reagents (Scheme 1).

The characterization of these compounds by any means other than crystallography is difficult as (i) microanalysis does not distinguish between mixtures of the component halides and a true adduct and (ii) nuclear magnetic resonance (NMR) does not help either as the only NMR signals are due to the phosphine ligands; similar comments also apply to **4**–**7**, below, with the exception of ^{119}Sn NMR singlets for **4**, **5**. However, it is notable that in **3**, for which two separate Me_3P environments might be expected, there is only one doublet in each of ^1H and ^{13}C NMR spectra and only one singlet in the ^{31}P NMR; that is, there is exchange in solution between phosphines attached to each of the two ions.

The structure of **1** is shown in Figure 1 and comprises what can viewed as a $[ZnCl_4]^{2-}$ anion bridging two $[(Ph_3P)_2Cu]^+$ cations in a μ_2, κ^2 manner; that is, the anion bridges two copper centers and simultaneously acts as a bidentate chelating ligand to each of them. The two unique Zn-Cl bonds [2.2709(5), 2.2902(5) Å] are close in length and shorter than the two Cu-Cl bonds [2.4555(5), 2.4535(5) Å], whereas each metal adopts a tetrahedral coordination sphere with significant distortion due to the chelating nature of the chlorines in $[ZnCl_4]^{2-}$ [∠ range: 101.647(16)°–123.294(17)°], and additionally, the bulky phosphines attached to the copper [∠ range: 92.154(16)°–129.91(2)°]. The two $CuCl_2Zn$ rings, which share a common zinc center, are planar and are twisted 75.52(1)° with respect to each other.

Surprisingly, in **2**, which incorporates a less bulky phosphine, the Cu_2Zn stoichiometry is retained, but copper only coordinates one group 15 donor and adopts a trigonal planar coordination (Figure 2). However, rather than forming a discrete molecular entity, the nominal $[ZnCl_4]^{2-}$ now acts in a μ_4-bridging mode to four separate copper centers and coordinates in a monodentate mode to each. The resulting structure is that of a one-dimensional polymer, in which eight-membered $Zn_2Cu_2Cl_4$ rings join at a common zinc center, with alternate rings being approximately orthogonal as a result of the tetrahedral geometry at zinc. In comparison with **1**, the $ZnCl_4$ unit is less regular, having two short [2.2563(6), 2.2547(6) Å] and two longer [2.2927(6), 2.2885(6) Å] Zn-Cl bonds. Similarly, the Cu-Cl [2.2688(6), 2.2639(6), 2.3710(6), 2.3849(6) Å] and Cu-P bonds [2.1913(6), 2.1772(6) Å] are shorter and less symmetric than in **1**, although to some extent this will be a natural result of the lower coordination number at copper. Free

$$ZnCl_2 + 2\ (Ph_3P)_2CuCl \xrightarrow{\text{toluene, 80°C, 4 h}} [(Ph_3P)_2CuCl]_2.ZnCl_2\ (\mathbf{1})$$

$$ZnCl_2 + 2\ CuCl + 4\ Me_3P \xrightarrow{\text{toluene, 60°C, 1 h}} \{[(Me_3P)CuCl]_2.ZnCl_2\}_n\ (\mathbf{2})$$

$$ZnCl_2 + 2\ CuCl + 6\ Me_3P \xrightarrow{\text{toluene, 60°C, 1 h}} [(Me_3P)_4Cu]^+[(Me_3P)_2Cu(Cl)_2ZnCl_2]^-\ (\mathbf{3})$$

Scheme 1

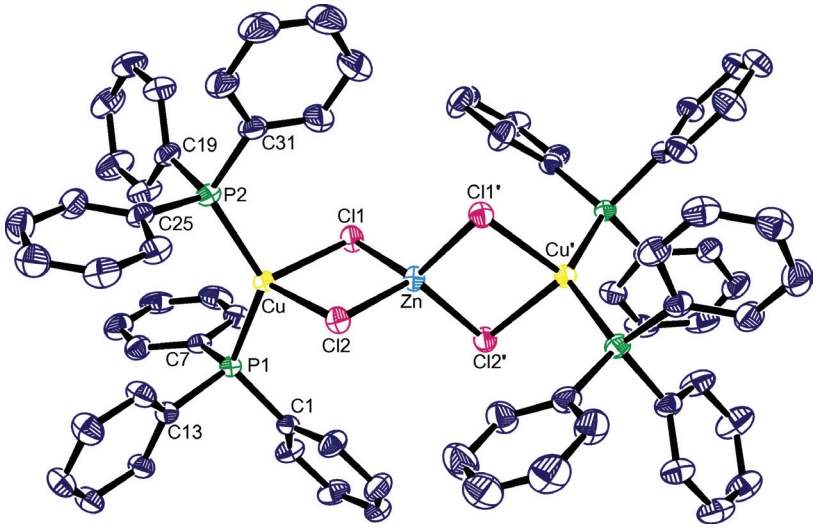

Figure 1 The asymmetric unit of **1** showing the labeling scheme used.
Thermal ellipsoids are at the 40% probability level. Only the α-carbons of the phenyl rings are numbered for clarity; hydrogen atoms have also been omitted. Selected geometric data: Zn-Cl(1) 2.2709(5), Zn-Cl(2) 2.2902(5), Cu-Cl(1) 2.4555(5), Cu-Cl(2) 2.4535(5), Cu-P(1) 2.2539(5), Cu-P(2) 2.2522(5) Å; Cl(1)-Zn-Cl(2) 101.647(16), Cl(1)-Zn-Cl(1′) 105.56(3), Cl(1)-Zn-Cl(2′) 123.294(17), Cl(2)-Zn-Cl(2′) 103.28(3), P(1)-Cu-P(2) 129.91(2), P(1)-Cu-Cl(1) 106.773(19), P(1)-Cu-Cl(2) 107.548(18), P(2)-Cu-Cl(1) 105.860(19), P(2)-Cu-Cl(2) 108.077(19), Cl(1)-Cu-Cl(2) 92.154(16), Zn-Cl(1)-Cu 83.228(16), Zn-Cl(2)-Cu 82.879(15)°. Symmetry operation: (′) 1-*x*, *y*, ½-*z*.

from its chelating role, the $ZnCl_4$ tetrahedron in **2** becomes markedly more regular [∠ range: 106.16(2)°–112.64(3)°]. To our knowledge, this polymeric arrangement is unique, with the closest comparison being that of the framework structure of $[H_3NMe]^+[Cu_2Zn_2Cl_7]^-$ (Martin et al., 1998).

The ionic product **3**, which results from a protocol that involves a larger quantity of phosphine than in the synthesis of **2**, retains a 2Cu:Zn ratio but is now formulated as a separated cation/anion pair: $[(Me_3P)_4Cu]^+[(Me_3P)_2Cu(Cl)_2ZnCl_2]^-$ (Figure 3). Although the tetrahedral cation is unremarkable, the anion can be viewed as half of that seen in **1**, but with differences. Whereas formally the anion can be viewed as $[ZnCl_4]^{2-}$ bonded to $[(Me_3P)_2Cu]^+$ by analogy to **1**, there is now marked asymmetry to the Zn-Cl

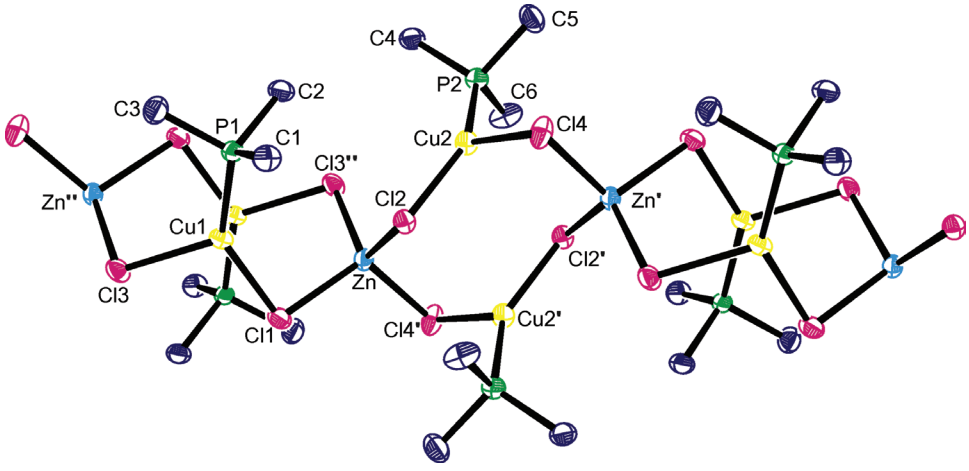

Figure 2 The asymmetric unit of **2** showing the labeling scheme used.
Thermal ellipsoids are at the 40% probability level; hydrogen atoms have been omitted for clarity. Selected geometric data: Zn-Cl(1) 2.2927(6), Zn-Cl(2) 2.2885(6), Zn-Cl(3″) 2.2563(6), Zn-Cl(4′) 2.2547(6), Cu(1)-P(1) 2.1913(6), Cu(1)-Cl(1) 2.2688(6), Cu(1)-Cl(3) 2.3710(6), Cu(2)-P(2) 2.1772(6), Cu(2)-Cl(2) 2.2639(6), Cu(2)-Cl(4) 2.3849(6) Å; Cl(1)-Zn-Cl(2) 106.16(2), Cl(1)-Zn-Cl(3″) 108.57(2), Cl(1)-Zn-Cl(4′) 108.46(3), Cl(2)-Zn-Cl(3″) 111.85(2), Cl(2)-Zn-Cl(4′) 108.89(2), Cl(3″)-Zn-Cl(4′) 112.64(3), P(1)-Cu(1)-Cl(1) 139.36(2), P(1)-Cu(1)-Cl(3) 117.88(3), Cl(1)-Cu(1)-Cl(3) 102.42(2), P(2)-Cu(2)-Cl(2) 142.64(2), P(2)-Cu(2)-Cl(4) 116.43(3), Cl(2)-Cu(2)-Cl(4) 100.85(2), Cu(1)-Cl(1)-Zn 96.04(2), Cu(2)-Cl(2)-Zn 103.99(2), Zn″-Cl(3)-Cu(1) 100.86(2), Zn′-Cl(4)-Cu(2) 93.02(2)°. Symmetry operations: (′) 1-*x*, 1-*y*,1-*z*; (″) 1-*x*, -*y*, 1-*z*.

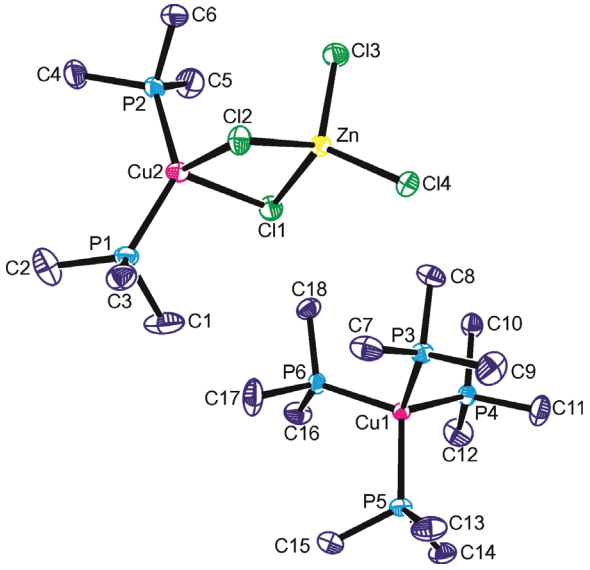

Figure 3 The asymmetric unit of **3** showing the labeling scheme used.
Thermal ellipsoids are at the 40% probability level; hydrogen atoms have been omitted for clarity. Selected geometric data: Zn-Cl(1) 2.3266(6), Zn-Cl(2) 2.3397(7), Zn-Cl(3) 2.2458(7), Zn-Cl(4) 2.2387(7), Cu(1)-P(3) 2.2716(6), Cu(1)-P(4) 2.2715(7), Cu(1)-P(5) 2.2721(7), Cu(1)-P(6) 2.2661(6), Cu(2)-Cl(1) 2.5024(7), Cu(2)-Cl(2) 2.4282(7), Cu(2)-P(1) 2.2227(7), Cu(2)-P(2) 2.2255(7) Å; Cl(1)-Zn-Cl(2) 96.70(2), Cl(1)-Zn-Cl(3) 109.73(3), Cl(1)-Zn-Cl(4) 115.91(3), Cl(2)-Zn-Cl(3) 111.37(3), Cl(2)-Zn-Cl(4) 110.22(3), Cl(3)-Zn-Cl(4) 111.98(3), Cl(1)-Cu(2)-Cl(2) 90.00(2), Cl(1)-Cu(2)-P(1) 105.53(3), Cl(1)-Cu(2)-P(2) 104.60(3), Cl(2)-Cu(2)-P(1) 107.26(3), Cl(2)-Cu(2)-P(2) 106.00(3), P(1)-Cu(2)-P(2) 134.51(3), Zn-Cl(1)-Cu(2) 82.45(2), Zn-Cl(2)-Cu(2) 83.81(2)°.

bonds with those to the terminal halogens being shorter [2.2458(7), 2.2387(7) Å] than those to the bridging chlorines [2.3266(6), 2.3397(7) Å], whereas the Cu-Cl bonds are also less symmetrical than in **1** [2.5024(7), 2.4282(7) Å]; moreover, the resulting $CuCl_2Zn$ ring is no longer planar. In comparison with **2**, the Cu-P bonds in the anion are longer [2.2227(7), 2.2255(7) Å], as might be expected from the enhanced coordination number in **3**, whereas the Cu-P bonds in the congested four-coordinate cation are longer still [2.2661(6)–2.2721(7) Å]. The $[(Me_3P)_4Cu]^+$ ion is well known and structures with a variety of counterions have been reported by others (Dempsey and Girolami, 1988; Chi et al., 1992; Eichhöfer et al., 1993; Pätow and Fenske, 2002; Schneider et al., 2007).

Cu-Sn bimetallic systems

Analogous reactions involving $SnCl_2$ and either preformed $(Ph_3P)_2CuCl$ or in a one-pot reaction with CuCl/Me_3P yielded the Cu-Cl-Sn heterobimetallic species **4** and **5** (Scheme 2).

$$SnCl_2 + (Ph_3P)_2CuCl \xrightarrow{\text{toluene, 80°C, } N_2} (Ph_3P)_2CuCl.SnCl_2 \quad (\mathbf{4})$$

$$SnCl_2 + CuCl + 2Me_3P \xrightarrow{\text{toluene, 60°C, } N_2} (Me_3P)_3CuSnCl_3 \quad (\mathbf{5})$$

Scheme 2

Compound **4** is a neutral 1:1 adduct (Figure 4) and is related to both **1** (but as an equivalent 1:1, rather than 2:1, adduct) and **3** (as a neutral equivalent). Compound **4** can be viewed as an $[SnCl_3]^-$ anion coordinating a $[(Ph_3P)_2Cu]^+$ cation, by analogy with **1** and **3**, but it is with the latter that the structural similarities are most striking. The Sn-Cl bonds divide into a short terminal [2.4562(12) Å] and longer bridging bonds to the μ_2-Cl [2.5402(10), 2.5680(11) Å], while the two Cu-Cl bonds [2.4516(11), 2.5052(12) Å] are asymmetric and closely parallel those in **3**, and the Cu-P bonds err marginally to the shorter side of those in **1** [2.2448(11), 2.2534(12) Å]; like **3**, the $CuCl_2Sn$ ring is nonplanar. The geometry at copper is a distorted tetrahedron, with an angle range that, not surprisingly, resembles that for **1** [∠ range: 88.67(4)°–135.81(4)°]. The $[SnCl_3]^-$ is trigonal pyramidal with a vacant area above the metal for a lone electron pair. What is interesting about the anion/cation relationship here, which is not seen in **1** (but is relevant to the antimony compound **7**, below), is the orientation of the phenyl ring attached to P(2) [C(19)-C(24)] with respect to tin (Figure 4). This ring sits above tin with Sn-C distances of 3.647(4)–4.043(4) Å and a Sn-ring centroid separation of 3.585 Å, distances that reflect a much weaker π-interaction than seen in examples where a more cationic tin is bonded to aromatic rings [usually, but not exclusively, solvent molecules (Probst et al., 1990) in $[MX_4]^-$ salts, M=B, X=C_6F_5 (Schafer et al., 2011), M=Al, X=Cl (Rodesiler et al., 1975; Weininger et al., 1979; Schmidbaur et al., 1989a,b,c, 1990b, 1991; Frank, 1990a,b), M=Ga, X=Cl (Frank, 1990c)], where the Sn-ring centroid is ca. 2.6 Å. It is similar to that in $\{Sn[S_2P(OPh)_2]_2\}_2$, where, as in **4**, the aromatic ring is part of an ancillary ligand (Sn-ring centroid 3.655 Å) (Lefferts et al., 1980). Interestingly, although all the C-C bonds within the C(19)-C(24) ring are equal within experimental error, those involving C(19), which is closest to tin [Sn-C(19) 3.647(4); C(19)-C(20) 1.393(6), C(19)-C(24) 1.398(6) Å], C(24) [Sn-C(24) 3.673(4) Å] and C(20) [Sn-C(20) 3.813(4); C(20)-C(21) 1.392(6) Å], err on the long side compared to the C-C bonds associated with longer Sn-C separations [1.372(6)–1.378(6) Å]. A more general review of p-block/arene compounds is available for the interested reader (Schmidbaur and Schier, 2008).

In contrast, the one-pot reaction involving Me_3P but retaining the reagent stoichiometry used to generate **4**

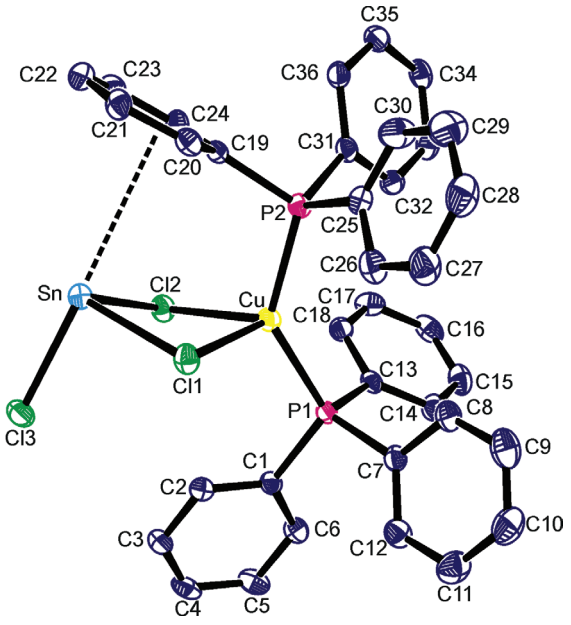

Figure 4 The asymmetric unit of **4** showing the labeling scheme used.
Thermal ellipsoids are at the 40% probability level. A co-crystallized toluene molecule has been omitted for clarity, as have the hydrogen atoms; C(33) is obscured by C(29). Selected geometric data: Sn-Cl(1) 2.5680(11), Sn-Cl(2) 2.5402(10), Sn-Cl(3) 2.4562(12), Sn-ring centroid 3.585, Cu-Cl(1) 2.4516(11), Cu-Cl(2) 2.5052(12), Cu-P(1) 2.2448(11), Cu-P(2) 2.2534(12) Å; Cl(1)-Sn-Cl(2) 85.40(3), Cl(1)-Sn-Cl(3) 92.89(4), Cl(2)-Sn-Cl(3) 92.68(4), Cl(1)-Cu-Cl(2) 88.67(4), Cl(1)-Cu-P(1) 111.16(4), Cl(1)-Cu-P(2) 100.74(4), Cl(2)-Cu-P(1) 103.47(4), Cl(2)-Cu-P(2) 107.15(4), P(1)-Cu-P(2) 135.81(4), Cu-Cl(1)-Sn 89.26(4), Cu-Cl(2)-Sn 88.72(3)°.

yields complex **5**, which incorporates a direct Sn-Cu bond (Figure 5). Compound **5** can again be viewed as a $[SnCl_3]^-$ anion coordinating a $[(Ph_3P)_3Cu]^+$ cation, but now coordination is *via* tin as a 2e donor rather than through halide bridges. As a consequence, there is an additional phosphine donor in **5** compared to **4** to maintain a tetrahedral geometry at copper. The Sn-Cu bond, which is not common, lies in the range 2.5662(14)–2.6160(15) Å across four independent molecules in the asymmetric unit and is longer than in $Ar(SiMe_3)SnCu(SiMe_3)$ ($Ar=C_6H_3Mes_2$-2,6) [2.4992(5)Å] (Klett et al., 1999) and $MeB[3\text{-}(CF_3)Pz]_3CuSn(Cl)$ (Bn_2ATI) (Pz=pyrazolyl, Bn_2ATI=*N*-benzyl-2-(benzylamino)-troponiminate) [2.4540(4)Å] (Dias et al., 2005), both of which incorporate Sn(II):→Cu(I) bonds, and that of a Sn(IV)-Cu(I) complex, $Ph_3SnCu(LPr)$ [LPr=1,3-bis(2,6-diisopropylphenyl)imidazol-2-ylidene)] [2.469(5) Å] (Bhattacharyya et al., 2008). The tetrahedral geometries at both tin and copper are largely unexceptional, save for the slightly narrower range of ∠Cl-Sn-Cl in **5** [95.75(13)°–96.39(12)°] compared to **4** [85.40(3)°–92.89(4)°], which may reflect the weak π-interaction in the latter.

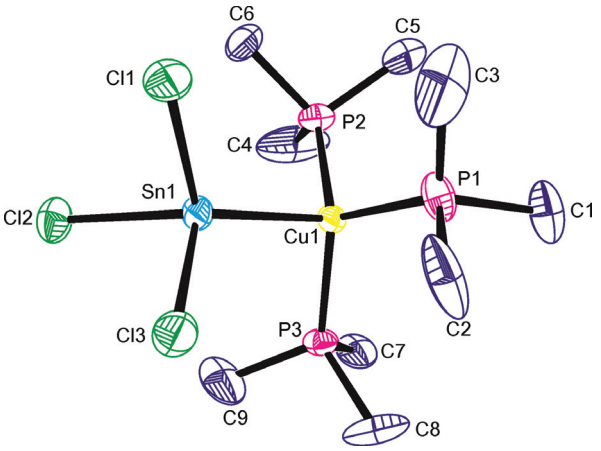

Figure 5 One of four similar molecules that constitute the asymmetric unit of **5** showing the labeling scheme used.
Thermal ellipsoids are at the 40% probability level; hydrogen atoms have been omitted for clarity. Selected geometric data: Sn(1)-Cu(1) 2.5997(14), Sn(1)-Cl(1) 2.435(3), Sn(1)-Cl(2) 2.426(3), Sn(1)-Cl(3) 2.444(3), Cu(1)-P(1) 2.264(3), Cu(1)-P(2) 2.242(3), Cu(1)-P(3) 2.250(3) Å; Cu(1)-Sn(1)-Cl(1) 120.33(9), Cu(1)-Sn(1)-Cl(2) 124.33(9), Cu(1)-Sn(1)-Cl(3) 117.90(10), Cl(1)-Sn(1)-Cl(2) 95.75(13), Cl(1)-Sn(1)-Cl(3) 95.89(14), Cl(2)-Sn(1)-Cl(3) 96.39(12), Sn(1)-Cu(1)-P(1) 98.55(10), Sn(1)-Cu(1)-P(2) 105.55(10), Sn(1)-Cu(1)-P(3) 101.99(8), P(1)-Cu(1)-P(2) 113.22(14), P(1)-Cu(1)-P(3) 117.41(15), P(2)-Cu(1)-P(3) 116.68(13)°.

Cu-Sb bimetallic systems

Following the approaches described above for Cu-Cl-Zn and Cu-Cl-Sn, Cu-Sb-Cl adducts were prepared similarly (Scheme 3):

When a 1:1 reaction stoichiometry is used, the product (**6**) is a 1:1 adduct, which, in keeping with the earlier discussions, can be thought of as the $[SbCl_4]^-$ anion coordinated to a $[(Ph_3P)_2Cu]^+$ cation. In the solid state, the molecule forms chlorine-bridged dimers to generate a five-coordinate square pyramidal geometry at antimony (τ=0.13) (Addison et al., 1984), while the familiar distorted tetrahedral geometry [∠ range: 81.91(2)°–124.46(3)°] is maintained at copper (Figure 6). However, bond length analysis suggests that the anion/cation association is the least appropriate description in this case. Thus, Cu-Cl(1) is the shortest of the Cu-Cl distances in the $(Ph_3P)_2Cu$ complexes studied [2.3129(7) Å], whereas the bond to the μ_2-Cl(2) is notably elongated [3.0070(9) Å]. Similarly, Cl(2) forms a short bond to antimony [2.3899(7) Å] and a much

$$SbCl_3 + (Ph_3P)_2CuCl \xrightarrow{\text{toluene, 80°C, } N_2} [(Ph_3P)_2CuCl.SbCl_3]_2 \quad (\mathbf{6})$$

$$SbCl_3 + 3(Ph_3P)_2CuCl \xrightarrow{\text{toluene, 80°C, } N_2} (Ph_3P)_3CuCl.SbCl_3 \quad (\mathbf{7})$$

Scheme 3

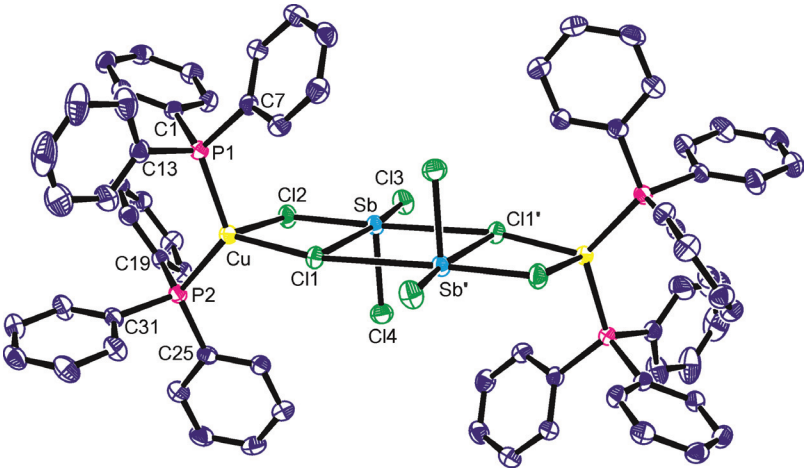

Figure 6 The asymmetric unit of **6** showing the labeling scheme used.
Thermal ellipsoids are at the 40% probability level. Only the α-carbons of the phenyl rings are shown for clarity, whereas hydrogen atoms have similarly been omitted. Selected geometric data: Sb-Cl(1) 3.0736(7), Sb-Cl(2) 2.3899(7), Sb-Cl(3) 2.3875(8), Sb-Cl(4) 2.3474(8), Sb-Cl(1′) 3.2106(6), Cu-Cl(1) 2.3129(7), Cu-Cl(2) 3.0070(9), Cu-P(1) 2.2701(8), Cu-P(2) 2.2668(8) Å; Cl(1)-Sb-Cl(2) 79.31(2), Cl(1)-Sb-Cl(3) 169.69(2), Cl(1)-Sb-Cl(4) 88.40(2), Cl(1)-Sb-Cl(1′) 100.202(16), Cl(2)-Sb-Cl(3) 90.44(3), Cl(2)-Sb-Cl(4) 95.63(3), Cl(2)-Sb-Cl(1′) 177.57(3), Cl(3)-Sb-Cl(4) 91.48(3), Cl(3)-Sb-Cl(1′) 90.08(2), Cl(4)-Sb-Cl(1′) 86.73(2), P(1)-Cu-Cl(1) 113.95(3), P(1)-Cu-Cl(2) 105.67(3), P(1)-Cu-P(2) 124.46(3), P(2)-Cu-Cl(1) 121.31(3), P(2)-Cu-Cl(2) 87.59(3), Cl(1)-Cu-Cl(2) 81.91(2), Cu-Cl(1)-Sb 98.88(2), Sb-Cl(2)-Cu 98.96(3)°. Symmetry operation: (′) 2-*x*, -*y*, 1-*z*.

weaker bridging bond to copper [3.0070(9) Å]. Thus, loose chlorine-bridged association between neutral $(Ph_3P)_2CuCl$ and $SbCl_3$ units is a more appropriate description here. Of the three chlorine atoms bonded to antimony, two are terminal [Sb-Cl(3) 2.3875(8); Sb-Cl(4) 2.3474(8) Å], one is μ_2-bridging between Sb and Cu [Cl(2)] and one is μ_3-bridging between two Sb atoms and one Cu atom [Cl(1)]. The weakness of the association between the heterometal units is reflected in the very short Sb-Cl(2) bond, which is very similar in length to the two terminal Sb-Cl bonds; dimerization by μ_2-Cl bridges between antimony centers is also weak [Sb-Cl(1′) 3.2106(6) Å]. The Cu-P distances are similar to those in **1** [2.2668(8), 2.2701(8) Å].

In contrast, when an excess of $(Ph_3P)_2CuCl$ is used in the reaction protocol, monomeric $[(Ph_3P)_3CuCl.SbCl_3]$ (**7**) is obtained (Figure 7). Compound **7** can be viewed as a $[SbCl_4]^-$ anion coordinated in a monodentate fashion to $[(Ph_3P)_3Cu]^+$ *via* a μ_2-Cl bridge. The Cu-Cl bond [2.4240(9) Å] is similar to those in **1** and **4** and elongated with respect to Cu-Cl(1) in **6**, whereas Sb-Cl(1) shows some lengthening [2.8005(9) Å] with respect to the three terminal Sb-Cl bonds [2.4473(10), 2.3549(11), 2.3474(10) Å] as a result of its bridging role; the four halogens then are more closely linked to antimony than copper. In addition to the μ_2-Cl, tetrahedral coordination at copper is completed by three Cu-P bonds, each of which is longer [2.3402(10), 2.3532(9), 2.3244(10) Å] than in the bis-triphenylphosphine complexes **1** and **4**, plausibly due to the steric crowding at copper from the three bulky donors. However, what is most interesting about this monomeric species is the role played by aromatic ring C(49)-C(54), which sits below antimony [Sb-C 3.468(4)–3.811(4); Sb-ring centroid 3.3323 (3) Å] in a manner analogous to that seen in

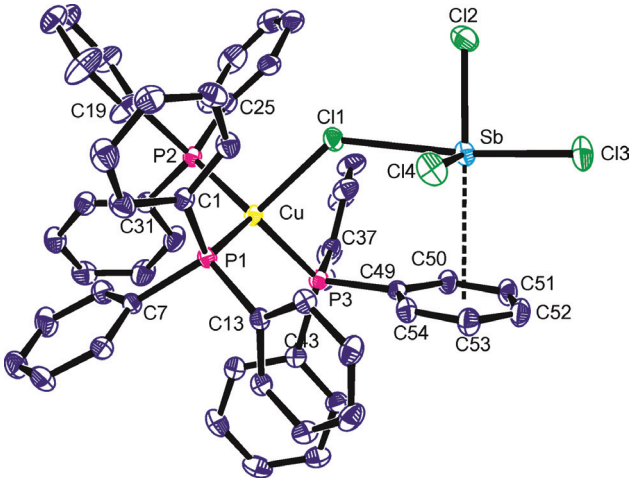

Figure 7 The asymmetric unit of **7** showing the labeling scheme used.
Thermal ellipsoids are at the 40% probability level. Only the α-carbons of the phenyl rings are numbered for clarity, except in the case of the ring π-bonded to antimony. Hydrogen atoms and the solvent have also been omitted. Selected geometric data: Sb-Cl(1) 2.8005(9), Sb-Cl(2) 2.3549(11), Sb-Cl(3) 2.4473(10), Sb-Cl(4) 2.3474(10), Sb-midpoint C(49)-C(54) 3.3323(3), Cu-Cl(1) 2.4240(9), Cu-P(1) 2.3402(10), Cu-P(2) 2.3532(9), Cu-P(3) 2.3244(10) Å; Cl(1)-Sb-Cl(2) 83.73(3), Cl(1)-Sb-Cl(3) 171.25(4), Cl(1)-Sb-Cl(4) 84.66(3), Cl(2)-Sb-Cl(3) 90.13(4), Cl(2)-Sb-Cl(4) 96.45(4), Cl(3)-Sb-Cl(4) 89.87(4), P(1)-Cu-P(2) 118.32(3), P(1)-Cu-P(3) 116.47(4), P(1)-Cu-Cl(1) 106.11(3), P(2)-Cu-P(3) 112.91(3), P(2)-Cu-Cl(1) 102.22(3), P(3)-Cu-Cl(1) 96.82(3), Cu-Cl(1)-Sb 131.71(4)°.

the tin complex **4**, generating a five-coordinated square-pyramidal geometry at antimony, with apical Cl(4) trans to the vacant space presumably occupied by the lone pair on Sb(III). Interactions between aromatic rings and antimony – so-called Menshutkin complexes (Schmidbaur and Schier, 2008) – have been previously reported in the structures of, for example, $SbCl_3 \cdot Et_6C_6$ (Schmidbaur et al., 1987), $SbBr_3$-9,10-dihydroanthracene (Schmidbaur et al., 1990a), $(MesSb)_4 \cdot C_6H_6$ (Ates et al., 1989), $SbCl_3$·1,4-bis(2-mercaptoethyl)benzene (Corinne et al., 2009) and a range of tethered diarenes (Burford et al., 1996) with widely differing Sb-ring centroid distances (ca. 2.9–3.8 Å) and arene hapticities (Schmidbaur and Schier, 2008). Furthermore, the π-interaction in η^3-(naphthalene)·$(SbCl_3)_2$ (Hulme and Szymanski, 1969) has been rationalized as donation of the π electrons of the arene ring into an empty orbital on antimony [originally described as an sp^3d^2 hydrid (Hulme and Szymanski, 1969) but most likely now to be seen as a σ* orbital], resulting in elongation of the Sb-Cl bond trans to the aromatic ring. In general, the interactions between group 15 elements and arenes have been rationalized in terms of a donor-acceptor interaction in which the arene is the donor (Schmidbaur and Schier, 2008). There is no indication among the C-C bonds of the C(49)-C(54) ring in **7** [1.380(5)–1.400(5) Å] of a π-arene interaction, although C(53), which sits diametrically opposite Cl(2) [∠Cl(2)-Sb…C(53) 176.7°], is involved in the two shortest measured C-C distances, and it is notable that the Sb-Cl(2) trans to the C(53) ring is the longest of the three terminal Sb-Cl bonds by ca. 0.1 Å. Furthermore, the point at which antimony makes an orthogonal contact with the C(49)-C(54) ring is displaced 0.471 Å away from the geometric center of the ring in the direction of C(53), from which we surmise that any π-arene…Sb bonding is, at most, η^3 in nature.

The reaction between $SbCl_3$ and Me_3P proved more difficult to elucidate. $SbCl_3$, CuCl and Me_3P (1:1:2) were heated to 60°C in toluene and left to cool slowly. Initially, the reaction yielded yellow crystals that were discovered to be twinned, so were redissolved at 100°C and cooled slowly to try to improve their quality. However, on cooling, a yellow precipitate remained with some colorless crystals on the side of the Schlenk flask which were structurally characterized as $[(Me_3P)_2Cu]^+[HPMe_3]_2^+[Sb_2Cl_9]^{3-}$ (**8**), which appears to be a minor hydrolysis product (Figure 8). From a repeat reaction, another minor product was obtained and structurally characterized as $[(Me_3P)_4Cu]^+[(Me_3P)_2Sb_2Cl_7]^-$ (**9**) (Figure 9) from a few colorless crystals found within the yellow product. Attempts to discover the nature of the major product in this reaction (the yellow precipitate) failed, as NMR could only confirm the presence of Me_3P groups and microanalysis proved inconclusive.

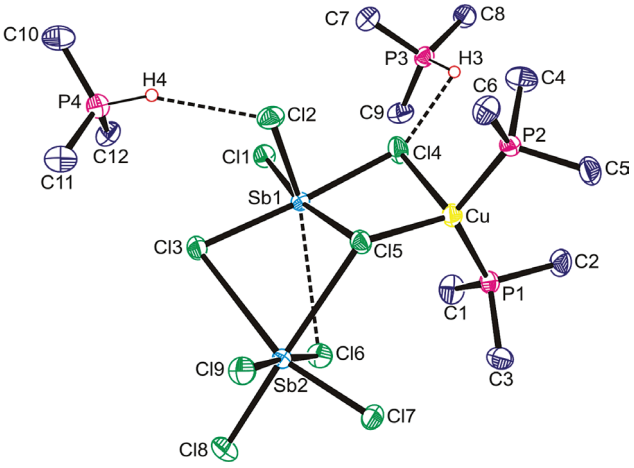

Figure 8 The asymmetric unit of **8** showing the labeling scheme used. Thermal ellipsoids are at the 40% probability level. Hydrogen atoms, except for those involved in hydrogen bonding, have been omitted for clarity. For selected geometric data, see Table 1. Hydrogen bond data: H(3)…Cl(4) 2.80(4), ∠P(3)-H(3)…Cl(4) 112(2); H(4)…Cl(2) 2.72(5), ∠P(4)-H(4)…Cl(2) 157(3)°.

Compound **8** consists of a bimetallic $[Sb_2Cl_9Cu(PPh_3)_2]^{2-}$ anion hydrogen-bonded to two $[Ph_3PH]^+$ cations [P(3)-H(3)…Cl(4): 2.80(4); P(4)-H(4)…Cl(2): 2.72(5) Å]. The

Table 1 Selected geometric data (Å, °) for **8**.

Bond lengths (Å)			
Sb(1)-Cl(1)	2.4441(10)	Sb(2)-Cl(6)	2.6163(11)
Sb(1)-Cl(2)	2.3741(11)	Sb(2)-Cl(7)	2.3893(10)
Sb(1)-Cl(3)	2.6327(10)	Sb(2)-Cl(8)	2.4196(11)
Sb(1)-Cl(4)	2.5907(10)	Sb(2)-Cl(9)	2.5890(11)
Sb(1)-Cl(5)	2.9692(10)	Sb(2)-Cl(3)	3.4951(11)
		Sb(2)-Cl(5)	3.0897(10)
Cu-Cl(4)	2.5931(12)	Cu-P(1)	2.2391(12)
Cu-Cl(5)	2.3979(11)	Cu-P(2)	2.2337(12)
Bond angles (°)			
Cl(1)-Sb(1)-Cl(2)	89.74(4)	Cl(3)-Sb(2)-Cl(5)	77.90(3)
Cl(1)-Sb(1)-Cl(3)	92.10(3)	Cl(6)-Sb(2)-Cl(3)	76.56(3)
Cl(1)-Sb(1)-Cl(4)	89.77(3)	Cl(6)-Sb(2)-Cl(5)	87.57(3)
Cl(1)-Sb(1)-Cl(5)	169.86(3)	Cl(6)-Sb(2)-Cl(7)	88.91(4)
Cl(2)-Sb(1)-Cl(3)	87.29(4)	Cl(6)-Sb(2)-Cl(8)	88.41(4)
Cl(2)-Sb(1)-Cl(4)	87.24(4)	Cl(6)-Sb(2)-Cl(9)	175.97(4)
Cl(2)-Sb(1)-Cl(5)	83.88(4)	Cl(7)-Sb(2)-Cl(3)	158.91(3)
Cl(3)-Sb(1)-Cl(4)	174.21(4)	Cl(7)-Sb(2)-Cl(5)	86.41(3)
Cl(3)-Sb(1)-Cl(5)	95.46(3)	Cl(7)-Sb(2)-Cl(8)	93.02(4)
Cl(4)-Sb(1)-Cl(5)	82.07(3)	Cl(7)-Sb(2)-Cl(9)	88.22(4)
P(1)-Cu-P(2)	122.80(4)	Cl(8)-Sb(2)-Cl(3)	101.64(3)
P(1)-Cu-Cl(4)	100.89(4)	Cl(8)-Sb(2)-Cl(5)	175.95(4)
P(1)-Cu-Cl(5)	117.57(4)	Cl(8)-Sb(2)-Cl(9)	88.91(4)
P(2)-Cu-Cl(4)	100.40(4)	Cl(9)-Sb(2)-Cl(3)	106.96(3)
P(2)-Cu-Cl(5)	112.92(4)	Cl(9)-Sb(2)-Cl(5)	95.08(3)
Cl(4)-Cu-Cl(5)	94.30(4)	Cu-Cl(5)-Sb(1)	90.90(3)
Sb(1)-Cl(3)-Sb(2)	82.96(3)	Cu-Cl(5)-Sb(2)	129.28(4)
Sb(1)-Cl(4)-Cu	90.90(3)	Sb(1)-Cl(5)-Sb(2)	85.40(3)

bimetallic anion is made up from $[Sb_2Cl_9]^{3-}$ coordinated to $[Cu(PPh_3)_2]^+$ in a κ^2-chelating mode through two chlorine atoms attached to a common antimony [Sb(1)], each of which bridges dissimilar metals in a μ_2-bridging manner. Although a limited number of other examples of $[Sb_2Cl_9]^{3-}$ have been structurally characterized (Ishihara et al., 1992; Willey et al., 1996; Wojtas and Jakubas, 2004; Gagor et al., 2008; Fu, 2010; Borisov et al., 2012), this is the first example of it acting as a ligand to coordinate another metal center. In **8**, copper again adopts a distorted tetrahedral coordination, in which the bond to the bridging Cl(5) [2.3979(11) Å] is shorter than that to the hydrogen-bonded Cl(4) [2.5931(12) Å]; in addition, the Cu-PMe_3 bonds are the longest noted in this study [2.2391(12), 2.2337(12) Å]. The $[Sb_2Cl_9]^{3-}$ moiety in **8** is considerably distorted in comparison with other examples of this anion as a result of its coordination to copper. The sum of the van der Waals radii for antimony and chlorine (ca. 3.95 Å, given Cl 1.75, Sb 2.20 Å) (Wells, 1984; Emsley, 1991) would allow for three μ_2-Cl bridges between the two group 15 elements in **8**, of which the bridge involving Cl(6) is notably longer [3.6159(12) Å] than those involving Cl(3) [3.4951(11) Å] or Cl(5) [3.0897(10) Å]; for comparison, the terminal Sb-Cl bonds lie in the range 2.3741(11)–2.5890(11) Å. In contrast, $[Me_3PH]^+_3$ $[Sb_2Cl_9]^{3-}$ adopts five phases, the most symmetrical of which has three identical terminal Sb-Cl bonds [2.421(4) Å] and three identical bridging interactions [2.9098(3) Å], which become progressively more asymmetric [typically Cl_t-Sb and Cl_b-Sb, ca. 2.41–2.54 and 2.69–2.85 Å] (Gagor et al., 2008), whereas when associated with protonated 1,4,7-trimethyl-1,4,7-triazacyclononane the ranges of Sb-Cl_t [2.373(4)–2.509(4) Å] and Sb-Cl_b [2.688(5)–3.532(5) Å] are more similar to those in **8** (Willey et al., 1996). Taking all the above Sb-Cl separations in **8** as bonds, the two antimony atoms adopt distorted octahedral geometries, with, in each case, one angle more open than expected to accommodate a lone electron pair [∠Cl(1)-Sb(1)-Cl(6) 115.48(3); [∠Cl(3)-Sb(2)-Cl(9) 106.96(3)°].

Like **3**, **9** contains the common $[(Me_3P)_4Cu]^+$ cation, which requires no further discussion. Uniquely, however, it also embodies the $[(Me_3P)_2Sb_2Cl_7]^-$ anion, for which there is no structural precedent (Figure 9), although the related $[Et_3PH]^+[(Et_3P)_2Sb_2Br_7]^-$ has been characterized (Clegg et al., 1994b). The closest structural comparison is with $[Ph_2Sb_2Cl_7]^{3-}$, which has a similar arrangement to **9** but which incorporates anionic phenyl groups rather than neutral phosphine donors (Sheldrick and Martin, 1992). Compound **9** has two anion/cation pairs in the asymmetric unit, and although these are nominally the same as that in $[Ph_2Sb_2Cl_7]^{3-}$, that is, the non-halogen substituents are cis to each other with respect to the Sb...Sb vector, all three anions are subtly different. $[Ph_2Sb_2Cl_7]^{3-}$ is the most regular, having just one μ_2-Cl bridge between metals, with two very similar Sb-Cl bonds [ca. 3.05 Å], and terminal Sb-Cl (2.443–2.532 Å) (two additional Sb-Cl_t at ca. 2.7 Å are involved in hydrogen bonds to a $[Me_3NH]^+$ counterion) (Sheldrick and Martin, 1992). In **9**, the $[(Me_3P)_2Sb_2Cl_7]^-$ anion based on Sb(1,2) also has only one μ_2-Cl bridge, but this is far more substantial [Sb-Cl(4) 2.8635(10), 2.8582(12) Å]; the Sb-Cl_t lie in the range 2.4567(13)–2.6553(11) Å,

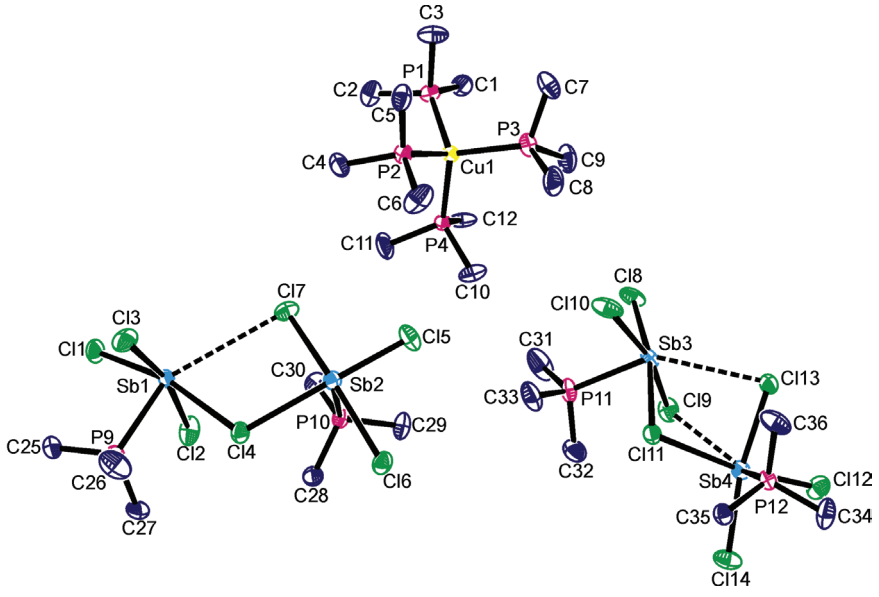

Figure 9 One of two $[(Me_3P)_4Cu]^+$ cations in the asymmetric unit of **8** showing the labeling scheme used.
Thermal ellipsoids are at the 40% probability level. Hydrogen atoms have been omitted for clarity. For selected geometric data, see Table 2.

Table 2 Selected geometric data (Å, °) for **9**.

Bond lengths (Å)			
Sb(1)-Cl(1)	2.4732(12)	Sb(3)-Cl(8)	2.5150(12)
Sb(1)-Cl(2)	2.5488(13)	Sb(3)-Cl(9)	2.6178(13)
Sb(1)-Cl(3)	2.6065(13)	Sb(3)-Cl(10)	2.5682(13)
Sb(1)-Cl(4)	2.8635(10)	Sb(3)-Cl(11)	2.7738(11)
Sb(1)-Cl(7)	3.7856(14)	Sb(3)-Cl(13)	3.5269(12)
Sb(2)-Cl(4)	2.8582(12)	Sb(4)-Cl(9)	3.6194(14)
Sb(2)-Cl(5)	2.4567(13)	Sb(4)-Cl(11)	3.0337(11)
Sb(2)-Cl(6)	2.6553(11)	Sb(4)-Cl(12)	2.4105(13)
Sb(2)-Cl(7)	2.5321(11)	Sb(4)-Cl(13)	2.5944(12)
Sb(1)-P(9)	2.5835(11)	Sb(4)-Cl(14)	2.5955(13)
Sb(2)-P(10)	2.5807(11)	Sb(3)-P(11)	2.5788(12)
		Sb(4)-P(12)	2.5855(11)
Cu(1)-P(1)	2.2651(12)	Cu(2)-P(5)	2.2680(11)
Cu(1)-P(2)	2.2723(12)	Cu(2)-P(6)	2.2652(11)
Cu(1)-P(3)	2.2722(13)	Cu(2)-P(7)	2.2550(12)
Cu(1)-P(4)	2.285(7)	Cu(2)-P(8)	2.2570(12)
Bond angles (°)			
Cl(1)-Sb(1)-Cl(2)	89.15(5)	Cl(4)-Sb(2)-Cl(5)	171.71(4)
Cl(1)-Sb(1)-Cl(3)	88.13(5)	Cl(4)-Sb(2)-Cl(6)	90.97(3)
Cl(1)-Sb(1)-Cl(4)	167.12(4)	Cl(4)-Sb(2)-Cl(7)	87.57(4)
Cl(1)-Sb(1)-Cl(7)	125.86(3)	Cl(4)-Sb(2)-P(10)	85.24(3)
Cl(1)-Sb(1)-P(9)	89.44(4)	Cl(5)-Sb(2)-Cl(6)	90.25(4)
Cl(2)-Sb(1)-Cl(3)	165.40(5)	Cl(5)-Sb(2)-Cl(7)	89.45(5)
Cl(2)-Sb(1)-Cl(4)	86.05(4)	Cl(5)-Sb(2)-P(10)	86.94(4)
Cl(2)-Sb(1)-Cl(7)	97.79(4)	Cl(6)-Sb(2)-Cl(7)	167.37(4)
Cl(2)-Sb(1)-P(9)	85.52(4)	Cl(6)-Sb(2)-P(10)	79.10(4)
Cl(3)-Sb(1)-Cl(4)	93.52(4)	Cl(7)-Sb(2)-P(10)	88.27(4)
Cl(3)-Sb(1)-Cl(7)	95.43(4)	Cl(4)-Sb(1)-P(9)	78.29(3)
Cl(3)-Sb(1)-P(9)	80.11(4)	Cl(7)-Sb(1)-P(9)	144.45(3)
Cl(4)-Sb(1)-Cl(7)	66.73(3)	Cl(9)-Sb(4)-Cl(11)	70.13(3)
Cl(8)-Sb(3)-Cl(9)	87.27(5)	Cl(9)-Sb(4)-Cl(12)	115.87(4)
Cl(8)-Sb(3)-Cl(10)	88.97(5)	Cl(9)-Sb(4)-Cl(13)	76.58(4)
Cl(8)-Sb(3)-Cl(11)	169.26(4)	Cl(9)-Sb(4)-Cl(14)	118.78(4)
Cl(8)-Sb(3)-Cl(13)	117.02(4)	Cl(9)-Sb(4)-P(12)	145.86(3)
Cl(8)-Sb(3)-P(11)	88.84(4)	Cl(11)-Sb(4)-Cl(12)	167.31(5)
Cl(9)-Sb(3)-Cl(10)	164.79(5)	Cl(11)-Sb(4)-Cl(13)	84.36(4)
Cl(9)-Sb(3)-Cl(11)	91.15(4)	Cl(11)-Sb(4)-Cl(14)	98.14(4)
Cl(9)-Sb(3)-Cl(13)	78.06(4)	Cl(11)-Sb(4)-P(12)	79.11(3)
Cl(9)-Sb(3)-P(11)	81.35(4)	Cl(12)-Sb(4)-Cl(13)	86.29(5)
Cl(10)-Sb(3)-Cl(11)	89.80(4)	Cl(12)-Sb(4)-Cl(14)	88.66(5)
Cl(10)-Sb(3)-Cl(13)	116.64(5)	Cl(12)-Sb(4)-P(12)	91.74(4)
Cl(10)-Sb(3)-P(11)	83.85(5)	Cl(13)-Sb(4)-Cl(14)	164.43(4)
Cl(11)-Sb(3)-Cl(13)	72.92(3)	Cl(13)-Sb(4)-P(12)	86.21(4)
Cl(11)-Sb(3)-P(11)	80.42(4)	Cl(14)-Sb(4)-P(12)	79.23(4)
Cl(13)-Sb(3)-P(11)	145.69(4)	Sb(3)-Cl(11)-Sb(4)	91.54(3)
Sb(2)-Cl(4)-Sb(1)	110.93(4)	Sb(4)-Cl(13)-Sb(3)	84.29(3)
Sb(2)-Cl(7)-Sb(1)	94.41(4)	Sb(3)-Cl(9)-Sb(4)	82.10(3)

and both metals adopt a square pyramidal geometry (τ= 0.03, 0.07). There is only one debatable long bond [Sb(1)-Cl(7) 3.7856(14) Å], which must be weak as Sb(2)-Cl(7) is relatively strong [2.5321(11) Å], but if real would serve to raise the geometry at Sb(1) to octahedral. For the anion involving Sb(3,4) the arrangement is closer to that of $[Sb_2Cl_9]^{3-}$ seen in **8** in having three μ_2-Cl bridges, each of which has one short and one longer interaction [Cl(9): 2.6178(13)/3.6194(14); Cl(11): 2.7738(11)/3.0337(11); Cl(13): 2.5944(12)/3.5269(12) Å]; of these, only those involving Cl(11) are comparable in symmetry to the μ_2-Cl bridge in the other $[(Me_3P)_2Sb_2Cl_7]^-$ anion, although the Sb-Cl_t are similar [2.4105(13)–2.5955(13) Å]. If all the μ_2-Cl bridges in this anion of **9** are considered valid interactions, then each antimony adopts a distorted octahedral geometry. Finally, it is notable that this is the only example coming from this study in which the phosphine has migrated from copper to the second metal center. Sb-P bonds are relatively common, and examples embracing simple R_3P-Sb coordination include $[\{(Me_3P)Ph_2Sb\}_4X]^{3+}[PF_6]_3^-$ (X=Cl, Br) (Wielandt et al., 2006), $[(Me_3P)_2SbCl_2]^+[CF_3SO_3]^-$ (Chitnis et al., 2011), $[(Ph_3P)_2Ph_2Sb]^+[PF_6]^-$ (Kilah et al., 2007) and $(Me_3P)_2Sb_2I_6$ (Clegg et al., 1994a).

Conclusions

Novel heterobimetallic M-Cl-M′ adducts (M, M′=Cu, Zn, Sn, Sb) have been prepared and structurally characterized. We have had no success in isolating clean products from the further nucleophilic substitution of Cl with, for example, SR^-, to generate M-S(R)-M′ precursors for CVD, which suggests that under the reaction conditions employed the adducts fragment. However, this work has shown that M-X-M′ can be made, and we have had more success in generating such M-S(R)-M′ species by direct assembly from, for example, $[Zn(SR)_3]^-$ and $(R_3P)_3CuCl$, details of which will form part of a separate report.

Experimental section

General procedures

All operations were performed under an atmosphere of dry argon using standard Schlenk line and glove box techniques. Toluene was dried using a commercially available solvent purification system (Innovative Technology Inc., MA, USA) and degassed under argon prior to use. Tetrahydrofuran (THF) was dried by refluxing over potassium before isolating by distillation and degassing under argon prior to use. Deuterated benzene (C_6D_6) and deuterated chloroform ($CDCl_3$) NMR solvents were purchased from Fluorochem (Hadfield, UK), and dried by refluxing over potassium and over 4 Å molecular sieves respectively, before isolating *via* vacuum distillation. All dry solvents were stored under argon in Young's ampoules over 4 Å molecular sieves.

Melting points were determined utilizing a Stuart SMP10 Melting Point Apparatus (Bibby Scientific Ltd, Stone, UK). Elemental analyses were performed externally by London Metropolitan University Elemental Analysis Service, UK. Solution ^1H, $^{13}C\{^1H\}$, $^{31}P\{^1H\}$ and $^{119}Sn\{^1H\}$ NMR spectra were recorded with a Bruker Avance 300

spectrometer (Brüker, Coventry, UK) at ambient temperature (25°C), save for the $^{119}Sn\{^{1}H\}$ NMR spectrum of **5**, which was recorded at 233 K on a Bruker Avance 400 spectrometer. ^{1}H and ^{13}C NMR chemical shifts are referenced internally to residual non-deuterated solvent resonances. All chemical shifts are reported in δ (ppm) and coupling constants in hertz. The following abbreviations are used: d (doublet), m (multiplet) and br (broad).

Synthesis of $[(Ph_3P)_2CuCl]_2.ZnCl_2$ (**1**): $(Ph_3P)_2CuCl$ (1.00 g, 1.61 mmol) and $ZnCl_2$ (0.11 g, 0.80 mmol) were stirred together in toluene (50 mL) at 80°C for 4 h. After 4 h, all solids had dissolved. White crystals were obtained on slow cooling of the solution to room temperature (0.97 g, 92%, mp 242–244°C). Analysis, found (calc. for $C_{72}H_{60}P_4Cl_4Cu_2Zn$): C 62.9 (62.7), H 4.44 (4.39). ^{1}H NMR (300 MHz, CD_2Cl_2) δ (ppm): 7.04–7.86 (m, Ph), ^{13}C NMR (300 MHz, CD_2Cl_2) δ (ppm): 134.5 (Ph), 133.0 (Ph), 130.4 (Ph), 129.18 (Ph), ^{31}P NMR (300 MHz, CD_2Cl_2) δ (ppm): -3.5.

Synthesis of $\{[(Me_3P)CuCl]_2.ZnCl_2\}_n$ (**2**): Me_3P (0.50 g, 6.57 mmol), CuCl (0.32 g, 3.29 mmol) and $ZnCl_2$ (0.22 g, 1.64 mmol) were stirred together in toluene (50 mL) at 60°C for 1 h. After 1 h, all solids had dissolved. White crystals were obtained on slow cooling of the solution to room temperature (0.42 g, 53%, mp 120–124°C). Analysis, found (calc. for $C_6H_{18}P_2Cl_4Cu_2Zn$): C 14.9 (15.0), H 3.62 (3.77). ^{1}H NMR (300 MHz, CD_2Cl_2) δ (ppm): 1.27 (d, *J*=6.03 Hz, Me), ^{13}C NMR (300 MHz, CD_2Cl_2) δ (ppm): 15.2 (d, *J*=19.9 Hz, Me), ^{31}P NMR (300 MHz, CD_2Cl_2) δ (ppm): -45.1.

Also prepared using the same method was $[(Me_3P)_4Cu]^+[(Me_3P)_2Cu(Cl)_2ZnCl_2]^-$ (**3**): Using Me_3P (0.75 g, 9.86 mmol), CuCl (0.32 g, 3.29 mmol) and $ZnCl_2$ (0.22 g, 1.64 mmol). White crystals were obtained on cooling the solution to -20°C (0.73 g, 56%, mp 74–75°C). Analysis, found (calc. for $C_{18}H_{54}P_6Cl_4Cu_2Zn$): C 26.5 (27.5), H 6.66 (6.92). ^{1}H NMR (300 MHz, CD_2Cl_2) δ (ppm): 1.27 (d, *J*=4.14 Hz, Me), ^{13}C NMR (300 MHz, CD_2Cl_2) δ (ppm): 15.4 (d, *J*=18.0 Hz, Me), ^{31}P NMR (300 MHz, CD_2Cl_2) δ (ppm): -45.3

Synthesis of $(Ph_3P)_2CuCl.SnCl_2$ (**4**): $(Ph_3P)_2CuCl$ (0.50 g, 0.80 mmol) and $SnCl_2$ (0.15 g, 0.80 mmol) were heated in toluene at 80°C for 4 h. Crystals were obtained on slow cooling of the solution to room temperature (0.52 g, 79%, mp 163–165°C). Analysis, found (calc. for $C_{36}H_{30}P_2Cl_3CuSn$): C 53.3 (53.2), H 3.85 (3.72). ^{1}H NMR (300 MHz, CD_2Cl_2) δ (ppm): 7.13–7.46 (m, Ph) ^{13}C NMR (300 MHz, CD_2Cl_2) δ (ppm): 134.4 (d, *J*=15.0 Hz, Ph), 132.1 (d, *J*=31.0 Hz, Ph), 130.9 (s, Ph), 129.5 (d, *J*=9.3 Hz, Ph) ^{31}P NMR (300 MHz, CD_2Cl_2) δ (ppm): -0.29 ^{119}Sn NMR (300 MHz, CD_2Cl_2) δ (ppm): -67.6 (br).

Also prepared using the same method was $(Me_3P)_3CuSnCl_3$ (**5**): Using Me_3P (0.50 g, 6.57 mmol), CuCl (0.32 g, 3.29 mmol) and $SnCl_2$ (0.62 g, 3.29 mmol) at 60°C, yielding 0.75 g, 66%, mp 205–207°C. Crystals suitable for diffraction were obtained by heating the solution to 100°C and cooling slowly in an oil bath. Analysis, found (calc. for $C_9H_{27}P_3Cl_3CuSn$): C 20.8 (20.9), H 5.34 (5.27). ^{1}H NMR (300 MHz, THF-d_8) δ (ppm): 1.36 (d, *J*=4.90 Hz) ^{13}C NMR (300 MHz, THF-d8) δ (ppm): 17.2 (d, *J*=18.6 Hz), ^{31}P NMR (300 MHz, THF-d_8) δ (ppm): -40.9, ^{119}Sn NMR (400 MHz, 233 K, THF-d^8) δ (ppm): -273.0 (br).

Synthesis of $[(Ph_3P)_2CuCl.SbCl_3]_2$ (**6**): $(Ph_3P)_2CuCl$ (0.50 g, 0.80 mmol) and $SbCl_3$ (0.18 g, 0.80 mmol) were stirred together in toluene (50 mL) at 80°C for 4 h. After 4 h, all solids had dissolved. After cooling to room temperature the solvent was removed *in vacuo* and the remaining white solid was redissolved in THF. Slow evaporation gave colorless crystals (0.61 g, 90%, mp 174–175°C). Analysis, found (calc. for $C_{36}H_{30}P_2Cl_4CuSb$): C 51.0 (51.0), H 3.68 (3.57). ^{1}H NMR (300 MHz, CD_2Cl_2) δ (ppm): 7.24–7.50 (m, Ph) ^{13}C NMR (300 MHz, CD_2Cl_2) δ (ppm): 134.4 (d, *J*=13.6 Hz, Ph), 132.1 (d, *J*=32.9 Hz, Ph), 131.0 (s, Ph), 129.5 (d, *J*=8.7 Hz, Ph) ^{31}P NMR (300 MHz, CD_2Cl_2) δ (ppm): -0.7.

Also prepared using the same method was $(Ph_3P)_3CuCl.SbCl_3$ (**7**): $(Ph_3P)_2CuCl$ (1.50 g, 2.40 mmol) and $SbCl_3$ (0.18 g, 0.80 mmol) yielding 0.76 g, 86%, mp 161–163°C on re-crystallization from toluene at -20°C. Analysis, found (calc. for $C_{54}H_{45}P_3Cl_4CuSb$): C 58.3 (58.4), H 4.14 (4.09). ^{1}H NMR (300 MHz, CD_2Cl_2) δ (ppm): 7.10–7.42 (m, Ph) ^{13}C NMR (300 MHz, CD_2Cl_2) δ (ppm): 134.4 (d, *J*=14.9 Hz, Ph), 132.1 (d, *J*=27.3 Hz, Ph), 130.5 (d, *J*=1.2 Hz, Ph), 129.2 (d, *J*=9.3 Hz, Ph) ^{31}P NMR (300 MHz, CD_2Cl_2) δ (ppm): -2.4.

Synthesis of $[(Me_3P)_2Cu]^+[HPMe_3]_2^+[Sb_2Cl_9]^{3-}$ (**8**): Me_3P (1 g, 13.14 mmol), CuCl (0.64 g, 6.58 mmol) and $SbCl_3$ (1.48 g, 6.58 mmol) were heated in toluene at 60°C for 1 h. Redissolving the yellow precipitate formed by heating to 100°C and leaving to cool slowly to room temperature produced a few colorless crystals, enough for X-ray crystallography, but no further analysis was carried out.

Also prepared using the same method was $[(Me_3P)_4Cu]^+[(Me_3P)_2Sb_2Cl_7]^-$ (**9**): Using Me_3P (1 g, 13.14 mmol), CuCl (0.64 g, 6.58 mmol) and $SbCl_3$ (1.48 g, 6.58 mmol). A few crystals suitable for diffraction were obtained by heating the solution to 100°C and cooling slowly in an oil bath, but no further analysis was carried out.

Crystallography

Experimental details relating to the single-crystal X-ray crystallographic studies are summarized in Table 3. For all structures, data were collected on a Nonius Kappa CCD diffractometer at 150(2) K using Mo-K_α radiation (λ=0.71073 Å). Structure solution followed by full-matrix least squares refinement was performed using the WinGX-1.70 suite of programs (Farrugia, 1999). Corrections for absorption (multiscan) were made in all cases.

Specific details: **1:** The asymmetric unit consists of half a complete molecular entity, the remainder generated by a crystallographic twofold axis coincident with the zinc center. Additionally, there are four toluene entities present, two of which [C(41)-C(47), C(51)-C(57)] straddle crystallographic twofold rotation axes and are hence disordered about same. The third region of solvent presents as half a molecule of toluene [C(71)-C(74)], which is proximate to an inversion center. This necessarily means that the methyl group position is disordered over two places on the phenyl ring. This solvent fragment is further disordered with a proximate half-occupancy toluene [C(61)-C(67)]. The level of disorder in this latter region of the electron density map necessitated the inclusion of some geometric restraints in order to assist convergence). **4**: Contains a molecule of lattice toluene. **5**: Satisfactory structure determination and refinement could only be brokered once pseudo-merohedral twinning (36%, about the 100 direct lattice direction) had been accounted for and the data were analyzed in space group *P*1 with four independent molecules in the asymmetric unit; ADP restraints were applied to three carbon atoms to assist convergence and some B alerts remain in the final cifcheck. The composition of the final product has, however, been unambiguously determined. **7**: The asymmetric unit includes 1.5 molecules of toluene. The toluene based on C(61)-C(67) is located close to a center of inversion and therefore has an occupation factor of 50%; toluene C(71)-C(77) is disordered in the ratio 1:1 and was isotropically refined, with a restraint applied to the C(71)-C(77) distance. All solvent C_6 phenyl rings were constrained to being ideal hexagons. **9**: The Me_3P moiety based on P(4) was seen to be disordered in a 70:30 ratio. P-C distances therein were refined subject to being similar, and some

Table 3 Crystallographic data for compounds **1–9**.

	1	**2**	**3**	**4**	**5**	**6**	**7**	**8**	**9**
Chemical formula	$C_{193}H_{175}Cl_8Cu_4P_8Zn_2$	$C_6H_{18}Cl_4Cu_2P_2Zn$	$C_{18}H_{54}Cl_4Cu_2P_6Zn$	$C_{43}H_{38}Cl_3CuP_2Sn$	$C_9H_{27}Cl_3CuP_3Sn$	$C_{36}H_{30}Cl_4CuP_2Sb$	$C_{129}H_{114}Cl_8Cu_2P_6Sb_2$	$C_{12}H_{38}Cl_9CuP_4Sb_2$	$C_{36}H_{108}Cl_{14}Cu_2P_{12}Sb_4$
Formula mass	3410.59	486.39	790.68	905.25	516.80	851.63	2504.20	932.39	2023.24
Crystal system	Monoclinic	Monoclinic	Triclinic	Orthorhombic	Triclinic	Triclinic	Monoclinic	Orthorhombic	Monoclinic
a (Å)	21.7997(4)	8.9728(2)	9.6824(2)	9.5878(1)	9.6870(4)	10.9622(4)	12.8356(1)	9.2897(1)	14.9358(1)
b (Å)	26.1254(5)	11.4549(3)	9.8414(2)	14.1197(2)	15.2860(6)	11.1033(4)	33.3653(3)	16.9124(2)	14.3309(1)
c (Å)	15.1684(2)	16.5345(3)	19.7345(4)	29.3342(5)	15.3330(4)	14.7604(6)	13.8224(1)	21.5525(3)	19.6701(2)
α (°)			89.0275(14)		101.575(2)	80.493(2)			
β (°)	102.863(1)	93.009(1)	83.5208(13)		106.412(2)	86.224(2)	95.532(1)		90.568(1)
γ (°)			87.3021(13)		90.762(1)	80.047(2)			
Unit cell volume (Å^3)	8422.0(2)	1697.11(7)	1866.26(7)	3971.17(10)	2127.71(13)	1743.96(11)	5892.06(8)	3386.14(7)	4210.05(6)
Space group	*C*2/*c*	$P2_1/n$	*P*-1	$P2_12_12_1$	*P*1	*P*-1	$P2_1/n$	$P2_12_12_1$	$P2_1$
Z	2	4	2	4	4	2	2	4	2
μ (Mo-kα) (mm^{-1})	1.032	4.674	2.318	1.477	2.759	1.808	1.121	3.110	2.458
Reflections measured	72 180	29 776	26 811	42 219	35 070	31 449	64 765	60 628	102 699
Independent reflections	9600	4975	8496	9001	35 086	7938	13 280	7721	24 569
R_{int}	0.0521	0.0619	0.0500	0.0844	0.0000	0.0861	0.0784	0.0618	0.0638
Final R_1 values [$I>2\sigma(I)$]	0.0323	0.0316	0.0338	0.0416	0.0762	0.0335	0.0479	0.0286	0.0391
Final $wR(F^2)$ values [$I>2\sigma(I)$]	0.0714	0.0716	0.0726	0.0767	0.2101	0.0642	0.0940	0.0573	0.0736
Final R_1 values (all data)	0.0552	0.0452	0.0547	0.0627	0.0947	0.0581	0.0986	0.0353	0.0680
Final $wR(F^2)$ values (all data)	0.0796	0.0772	0.0795	0.0844	0.2270	0.0721	0.1101	0.0599	0.0827
Goodness of fit on F^2	1.013	1.073	1.028	1.033	1.043	1.061	1.019	1.089	1.019
Flack parameter				-0.009(14)	0.15(2)			-0.017(13)	-0.020(8)
Largest diff. peak and hole (eÅ^{-3})	0.320, -0.319	0.613, -0.897	0.427, -0.597	0.997, -0.859	3.916, -2.433	0.741, -0.736	0.706, -0.753	0.741, -0.736	0.856, -1.257

ADP restraints were added to the fractional occupancy carbons to assist convergence.

Supporting information

Crystallographic data for the structural analysis (in CIF format) have been deposited with the Cambridge Crystallographic Data Centre, CCDC nos. 970317–970325 for **1**–**9**, respectively. Copies of this information may be obtained from the Director, CCDC, 12 Union Road, Cambridge CB21EZ, UK (Fax: +44-1233-336033; e-mail: deposit@ccdc.cam.ac.uk or www.ccdc.cam.ac.uk).

Acknowledgments: We thank the EPSRC for financial support through the PV21 Supergen program, and Stephen Boyer, London Metropolitan University, UK, for performing the microanalyses.

Received November 18, 2013; accepted January 20, 2014; previously published online March 10, 2014

References

Abermann, S. Non-vacuum processed next generation thin film photovoltaics: towards marketable efficiency and production of CZTS based solar cells. *Sol. Energy* **2013**, *94*, 37–70.

Addison, A. W.; Rao, T. N.; Reedijk, J.; van Rijn, J. Verschoor, G. C. Synthesis, structure, and spectroscopic properties of copper(II) compounds containing nitrogen-sulphur donor ligands; the crystal and molecular structure of aqua[l,7-bis(n-methylbenzimidazol-2′-yl)-2,6-dithiaheptane]copper(II) perchlorate. *J. Chem. Soc., Dalton Trans.* **1984**, *13*, 1349–1356.

Ates, M.; Breunig, H. J.; Gulec, S.; Offermann, W.; Haberle, K.; Drager, M. Syntheses and structures of ethyl-, propyl-, butyl-, and mesitylantimony. *Chem. Ber.* **1989**, *122*, 473–478.

Bhattacharyya, K. X.; Akana, J. A.; Laitar, D. S.; Berlin, J. M.; Sadighi, J. P. Carbon-carbon bond formation on reaction of a copper(I) stannyl complex with carbon dioxide. *Organometallics* **2008**, *27*, 2682–2684.

Borisov, A. V.; Matsulevich, Zh. V.; Osmanov, V. K.; Borisova, G. N.; Mamedova, G. Z.; Magerramov, A. M.; Khrustalev, B. N. Sulfenyl halides in the synthesis of heterocycles. 4. Heterocyclization in reactions of alkenes with sulfenylating reagents based on di(2-pyridyl) disulfide. *Chem. Heterocycl. Compd.* **2012**, *48*, 1098–1104.

Burford, N.; Clyburne, J. A. C.; Wiles, J. A.; Cameron, T. S.; Robertson, K. N. Tethered diarenes as four-site donors to $SbCl_3$. *Organometallics* **1996**, *15*, 361–364.

Chi, K.-M.; Farkas, J.; Hampden-Smith, M. J.; Kodas, T. T.; Duesler, E. N. The chemistry of copper(I) β-diketonate compounds. Part 4. Synthesis and characterization of $CuXl_n$(x=β-diketonate or Cl, l=PMe_3, n=2 or 4; l=PEt_3, n=2). *J. Chem. Soc., Dalton Trans.* **1992**, *21*, 3111–3117.

Chino, K.; Koike, J.; Eguchi, S.; Araki, H.; Nakamura, R.; Jimbo, K. Katagiri, H. Preparation of Cu_2SnS_3 thin films by sulfurization of Cu/Sn stacked precursors. *Jpn. J. Appl. Phys.* **2012**, *51*, 10NC35/1.

Chitnis, S. S.; Peters, B.; Conrad, E.; Burford, N.; McDonald, R.; Ferguson, M. J. Structural diversity for phosphine complexes of stibenium and stibinidenium cations. *Chem. Commun.* **2011**, *47*, 12331–12333.

Clegg, W.; Elsegood, M. R. J.; Graham, V.; Norman, N. C.; Pickett, N. L.; Tavakkoli, K. Neutral phosphine complexes of antimony(III) and bismuth(III) halides. *J. Chem. Soc., Dalton Trans.* **1994a**, *23*, 1743–1751.

Clegg, W.; Elsegood, M. R. J.; Norman, N. C.; Pickett, N. L. Anionic phosphine complexes of antimony(III) and bismuth(III) halogenoanions. *J. Chem. Soc., Dalton Trans.* **1994b**, *23*, 1753–1757.

Corinne, A. A.; Virginia, M. C.; Lev, N. Z.; Darren, W. J. Supramolecular organization using multiple secondary bonding interactions. *Cryst. Growth Des.* **2009**, *9*, 3011–3013.

Curtis, N. F.; Gladkikh, O. P. A copper(II) compound of a tetradentate amine imine ligand with coordinated tetrachlorozincate ion. *Aust. J. Chem.* **2000**, *53*, 597–600.

Dempsey, D. F.; Girolami, G. S. Copper(I) alkyls. Synthesis and characterization of tertiary phosphine adducts and the crystal structure of the dimethylcuprate complex $[Cu(PMe_3)_4][CuMe_2]$. *Organometallics* **1988**, *7*, 1208–1213.

Dias, H. V. R.; Wang, X.; Diyabalanage, H. V. K. Fluorinated tris(pyrazolyl)borate ligands without the problematic hydride moiety: isolation of copper(I) ethylene and copper(I)-tin(II) complexes using $[MeB(3\text{-}(CF_3)pz)_3]^-$. *Inorg. Chem.* **2005**, *44*, 7322–7324.

Dufton, J. T. R.; Walsh, A.; Panchmatia, P. M.; Peter, L. M.; Colombara, D.; Islam, M. S. Structural and electronic properties of $CuSbS_2$ and $CuBiS_2$: potential absorber materials for thin-film solar cells. *Phys. Chem. Chem. Phys.* **2012**, *14*, 7229–7233.

Eichhöfer, A.; Fenske, D.; Holstein, W. New phosphido-bridging copper clusters. *Angew. Chem., Int. Ed.* **1993**, *32*, 242–245.

Emsley, J. The Elements, 2nd Edition; Clarendon Press: Oxford, 1991.

Ennaoui, A.; Lux-Steiner, M.; Weber, A.; Abou-Ras, D.; Koetschau, I.; Schock, H. W.; Schurr, R.; Hoelzing, A.; Jost, S.; Hock, R.; et al. Cu_2ZnSnS_4 thin film solar cells from electroplated precursors: novel low-cost perspective. *Thin Solid Films* **2009**, *517*, 2511–2514.

Farrugia, L. J. Wingx: suite for small-molecule single-crystal crystallography. *J. Appl. Crystallogr.* **1999**, *32*, 837–838.

Frank, W. Catena-(tetrakis(μ_2-chloro)-chloro-(η^6-p-toluene)-aluminium-tin(II)). *Z. Anorg. Allg. Chem.* **1990a**, *585*, 121.

Frank, W. Schwermetall-π-komplexe. III. Darstellung, eigenschaften und kristallstrukturen von α- und β-(toluolSnCl)($AlCl_4$) sowie (mesitylenSnCl)($AlCl_4$) zur abhängigkeit der aren-metall-bindungsstärke von der arenbasizität. *Z. Anorg. Allg. Chem.* **1990b**, *585*, 121–141.

Frank, W. Schwermetall-π-komplexe, V. Das schichtenpolymer {([C_6H_6SnCl][$GaCl_4$])$_2$}x,y. *Chem. Ber.* **1990c**, *123*, 1233–1237.

Fu, X.-Q. Hexakis(4-acetylpyridinium) bis((c-chloro)-octachloro-diantimonate(III)). *Acta Crystallogr., Sect. E: Struct. Rep. Online* **2010**, *66*, m736.

Gagor, A.; Wojtas, M.; Pietraszko, A.; Jakubas, R. Tris(trimethylphosphonium)(μ_2-chloro)-octachloro-di-antimony(III). *Acta Crystallogr., Sect. B: Struct. Sci.* **2008**, *64*, 558–566.

Gardberg, A. S.; Ibers, J. A. *trans*-Bis(hexafluoroantimonato) (phthalocyaninato)copper(II). *Acta Crystallogr., Sect. C: Cryst. Struct. Commun.* 2001, *57*, 528–529.

Gladkikh, O. P.; Curtis, N. F.; Heath, S. L. μ-Chloro-1:2κ^2Cl-trichloro-2κ^3Cl-(2,4-dimethyl-5,8-diazadec-4-ene-2,10-diamine-1κ^4*N,N′,N″,N‴*)copper(II)zinc(II). *Acta Crystallogr., Sect. C: Cryst. Struct. Commun.* **1997**, *53*, 197–200.

Gou, S.-H.; Xu, Z.; You, X.-Z.; Zheng, P.-J.; Dong, J. Synthesis and crystal structure of a new polynuclear complex with a monomer of (3,4,9,10-dibenzo-1,12-diaza-5,8-dioxacyclopentadecane)-copper(II)(μ-C1)$_2$zinc(II) chloride *Chin. J. Chem.* **1992**, *10*, 232–236.

Guan, H.; Shen, H.; Gao, C.; He, X. Structural and optical properties of Cu_2SnS_3 and Cu_3SnS_4 thin films by successive ionic layer adsorption and reaction. *J. Mater. Sci. - Mater. Electron.* **2013**, *24*, 1490–1494.

Han, Y.-G.; Xu, C.; Duan, T.; Wu, F.-H.; Zhang, Q.-F.; Leung, W.-H. Heterometallic aggregates of copper(I) with metalloligand Sn(edt)$_2$ (edt=ethane-1,2-dithiolate): syntheses and structures of [Sn(edt)$_2$Cl(μ-I)(μ_3-I)($CuPPh_3$)$_3$], [Sn(edt)$_2$(μ-Br)$_2$(μ_3-Br)$_2$($CuPPh_3$)$_4$], and [{Sn(edt)$_2$}$_3$(μ-OH)$_3$$Cu_5$($PPh_3$)$_8$][$PF_6$]$_2$. *Inorg. Chem.* **2009**, *48*, 8796–8802.

Hulme, R.; Szymanski, J. T. The crystal structure of the 2:1 complex between antimony trichloride and naphthalene. *Acta Crystallogr., Sect. B: Struct. Sci.* **1969**, *B25*, 753–761.

Ishihara, H.; Watanabe, K.; Iwata, A.; Yamada, K.; Kinoshita, Y.; Okuda, T.; Krishnan, V. G.; Dou, S.-Q.; Weiss, A. NQR and X-ray studies of [$N(CH_3)_4$]$_3$$M_2X_9$ and (CH_3NH_3)$_3$$M_2X_9$ (M=Sb, Bi; X=Cl, Br). *Z. Naturforsch., A: Phys. Sci.* **1992**, *47*, 65–74.

Ito, K. Nakazawa, T. Electrical and optical-properties of stannite-type quaternary semiconductor thin-films. *Jpn. J. Appl. Phys. Part 1* **1988**, *27*, 2094–2097.

Kilah, N. L.; Petrie, S.; Stranger, R.; Wielandt, J. W.; Willis, A. C.; Wild, S. B. Triphenylphosphine-stabilized diphenyl-arsenium, -stibenium, and -bismuthenium salts. *Organometallics* **2007**, *26*, 6106–6113.

Klett, J.; Klinkhammer, K. W.; Niemeyer, M. Ligand exchange between arylcopper compounds and bis(hypersilyl)tin or bis(hypersilyl)lead: synthesis and characterization of hypersilylcopper and a stannanediyl complex with a Cu-Sn bond. *Chem. - Eur. J.* **1999**, *5*, 2531–2536.

Kociok-Köhn, G.; Molloy, K. C; Sudlow, A. L. Molecular routes to Cu_2ZnSnS_4: a comparison of approaches to bulk and thin-film materials. *Can. J. Chem.* **2013**, accepted for publication.

Koike, J.; Chino, K.; Aihara, N.; Araki, H.; Nakamura, R.; Jimbo, K.; Katagiri, H. Cu_2SnS_3 thin-film solar cells from electroplated precursors. *Jpn. J. Appl. Phys.* **2012**, *51*, 10NC34/1.

Kurihara, M.; Berg, D.; Fischer, J.; Siebentritt, S.; Dale, P. J. Kesterite absorber layer uniformity from electrodeposited precursors. *Phys. Status Solidi C* **2009**, *6*, 1241–1244.

Lazcano, Y. R.; Nair, M. T. S.; Nair, P. K. $CuSbS_2$ thin film formed through annealing chemically deposited Sb_2S_3-CuS thin films. *J. Cryst. Growth* **2001**, *223*, 399–406.

Lefferts, J. L.; Hossain, M. B.; Molloy, K. C.; Helm, D. v. d.; Zuckerman, J. J. Bis((μ_2-O,O′-diphenyldithiophosphato-S,S,S′)-(O,O′-diphenyldithiophosphato-S,S′)-di-tin(II)). *Angew. Chem., Int. Ed.* **1980**, *19*, 309.

Mandal, S. K.; Thompson, L. K.; Gabe, E. J.; Charland, J.-P.; Lee, F. L. Binuclear complexes of the ligand 3,6-bis(2-pyridylthio) pyridazine involving homo- and heterodiatomic binuclear centers (Cu-Cu, Cu-Co, Cu-Zn). Crystal structure of bis[μ-3,6-bis(2-pyridylthio)pyridazine-N1, μ-N2, μ-N3, N4](μ-chloro)dicopper(II) triperchlorate-acetonitrile. *Inorg. Chem.* **1988**, *27*, 855–859.

Manolache, S.; Duta, A. The influence of the spray deposition parameters in the photovoltaic response of the three-dimensional (3-D) solar cell: TCO/dense TiO_2/$CuSbS_2$/graphite. *J. Optoelectron. Adv. M.* **2007**, *9*, 3219–3222.

Manolache, S.; Duta, A.; Isac, L.; Nanu, M.; Goossens, A. Schoonman, J. The influence of the precursor concentration on $CuSbS_2$ thin films deposited from aqueous solutions. *Thin Solid Films* **2007**, *515*, 5957–5960.

Manson, J. L.; Schlueter, J. A.; Funk, K. A.; Southerland, H. I.; Twamley, B.; Lancaster, T.; Blundell, S. J.; Baker, P. J.; Pratt, F. L.; Singleton, J.; et al. Strong H…F hydrogen bonds as synthons in polymeric quantum magnets: structural, magnetic, and theoretical characterization of [Cu(HF_2)(pyrazine)$_2$]SbF_6, [Cu_2F(HF)(HF_2)(pyrazine)$_4$](SbF_6)$_2$, and [CuAg(H_3F_4)(pyrazine)$_5$](SbF_6)$_2$. *J. Am. Chem. Soc.* **2009**, *131*, 6733–6747.

Margulieux, K. R.; Sun, C.; Zakharov, L. N.; Holland, A. W.; Pak, J. J. Stepwise introduction of thiolates in copper-indium binuclear complexes. *Inorg. Chem.* **2010**, *49*, 3959–3961.

Martin, J. D.; Dattelbaum, A. M.; Thornton, T. A.; Sullivan, R. M.; Yang, J.; Peachey, M. T. Metal halide analogues of chalcogenides: a building block approach to the rational synthesis of solid-state materials. *Chem. Mater.* **1998**, *10*, 2699–2713.

Moriya, K.; Watabe, J.; Tanaka, K. Uchiki, H. Characterization of Cu_2ZnSnS_4 thin films prepared by photo-chemical deposition. *Phys. Status Solidi C* **2006**, *3*, 2848–2852.

Moriya, K.; Tanaka, K.; Uchiki, H. Fabrication of Cu_2ZnSnS_4 thin-film solar cell prepared by pulsed laser deposition. *Jpn. J. Appl. Phys* **2007**, *46*, 5780–5781.

Nair, M. T. S.; Rodriguez-Lazcano, Y.; Pena, Y.; Messina, S.; Campos, J.; Nair, P. K. Absorber films of antimony chalcogenides via chemical deposition for photovoltaic application. *Mater. Res. Soc. Symp. Proc.* **2005**, *836*, 167–172.

Nakajima, Y.; Shiraishi, Y.; Tsuchimoto, T.; Ozawa, F. Synthesis and coordination behavior of CuI bis(phosphaethenyl)pyridine complexes. *Chem. Commun.* **2011**, *47*, 6332–6334.

Nakamura, Y.; Yonemura, M.; Arimura, K.; Usuki, N.; Ohba, M.; Okawa, H. Tetranuclear mixed-metal $M^{II}_2Cu^{II}_2$ complexes derived from a phenol-based macrocyclic ligand having two N(amine)$_2$O$_2$ and two N(imine)$_2$O$_2$ metal-binding sites. *Inorg. Chem.* **2001**, *40*, 3739–3744.

Nakayama, N.; Ito, K. Sprayed films of stannite Cu_2ZnSnS_4. *Appl. Surf. Sci.* **1996**, *92*, 171–175.

Nayek, H. P.; Massa, W.; Dehnen, S. A heterometallic, heterovalent CuI/SnII/IV/S cluster with an unprecedented Cu_4Sn core and stannacyclopentane units. *Inorg. Chem.* **2008**, *47*, 9146–9148.

Park, J.; Song, M.; Jung, W. M.; Lee, W. Y.; Kim, H.; Kim, Y.; Hwang, C.; Shim, I.-W. Syntheses of Cu_2SnS_3 and Cu_2ZnSnS_4

nanoparticles with tunable Zn/Sn ratios under multibubble sonoluminescence conditions. *Dalton Trans.* **2013**, *42*, 10545–10550.

Pätow, R.; Fenske, D. Synthesen und kristallstrukturen von Cu- und Ag-komplexen mit $[Ta_6S_{17}]^{4-}$-ionen als liganden. *Z. Anorg. Allg. Chem.* **2002**, *628*, 2790–2794.

Prins, R.; Biagini-Cingi, M.; Drillon, M.; de Graaf, R. A. G.; Haasnoot, J.; Manotti-Lanfredi, A.-M.; Rabu, P.; Reedijk, J.; Ugozzoli, F. Trinuclear copper(II) coordination compounds with the new ligand 1,9-bis-(3-amino-4*H*-1,2,4-triazol-5-yl)-3,7-dithianonane; X-ray structures and magnetochemistry *Inorg. Chim. Acta* **1996**, *248*, 35–44.

Probst, T.; Steigelmann, O.; Riede, J.; Schmidbaur, H. Ge(II) and Sn(II) complexes of [2.2.2]paracyclophane with threefold internal η^6 coordination. *Angew. Chem., Int. Ed.* **1990**, *29*, 1397–1398.

Pryma, O. V.; Petrusenko, S. R.; Kokozay, V. N.; Skelton, B. W.; Shishkin, O. V.; Teplytska, T. S. A facile direct synthesis of bimetallic Cu(II)Zn(II) complexes with ethylenediamine revealing different types of chain crystal structures *Eur. J. Inorg. Chem.* **2003**, 1426–1432.

Ramasamy, K.; Malik, M. A.; O'Brien, P. The chemical vapour deposition of Cu_2ZnSnS_4 thin films. *Chem. Sci.* **2012**, *48*, 5703.

Rodesiler, P. F.; Auel, T.; Amma, E. L. Metal ion-aromatic complexes. XXII. Preparation, structure, and stereochemistry of tin(II) in π-benzenetin di(tetrachloroaluminate)-benzene. *J. Am. Chem. Soc.* **1975**, *97*, 7405–7410.

Schafer, A.; Winter, F.; Saak, W.; Haase, D.; Pottgen, R.; Muller, T. Stannylium ions, a tin(II) arene complex, and a tin dication stabilized by weakly coordinating anions. *Chem.-Eur. J.* **2011**, *17*, 10979–10984.

Schmidbaur, H.; Schier, A. π-Complexation of post-transition metals by neutral aromatic hydrocarbons: the road from observations in the 19th century to new aspects of supramolecular chemistry. *Organometallics* **2008**, *27*, 2361–2395.

Schmidbaur, H.; Nowak, R.; Huber, B.; Mueller, G. Hexaethylbenzene-trichloroantimony: a Menshutkin complex with a centroid antimony-arene coordination. *Organometallics* **1987**, *6*, 2266–2267.

Schmidbaur, H.; Probst, T.; Huber, B.; Muller, G.; Kruger, C. Aromaten-komplexe der p-block-elemente: eine tetramere η^6-koordinationsverbindung des hexamethylbenzols mit $Sn(AlCl_4)Cl$ und kristall-chlorbenzol. *J. Organomet. Chem.* **1989a**, *365*, 53–60.

Schmidbaur, H.; Probst, T.; Huber, B.; Steigelmann, O.; Muller, G. Arene complexes of p-block elements: $[(\eta^6\text{-}C_6H_6)_2SnCl(AlCl_4)]_2$. The first bis(arene) coordination compound of a group 14 element. *Organometallics* **1989b**, *8*, 1567–1569.

Schmidbaur, H.; Probst, T.; Steigelmann, O.; Muller. π-Complexes of p-block elements: $[(\eta^6\text{-}C_6Me_6)Sn(AlCl_4)_2]_2.3C_6H_6$ – a dimeric coordination compound of hexamethylbenzene with $Sn(AlCl_4)_2$. *Z. Naturforsch., B: Chem. Sci.* **1989c**, *44*, 1175.

Schmidbaur, H.; Nowak, R.; Steigelmann, O.; Muller, G. π-Complexes of p-block elements: planar dihydroanthracene in a Menshutkin complex. Crystal structure of $Br_3Sb{\cdot}C_6H_4(CH_2)_2C_6H_4{\cdot}SbBr_3$. *Chem. Ber.* **1990a**, *123*, 19–22.

Schmidbaur, H.; Probst, T.; Steigelmann, O.; Muller, G. π-Complexes of p-block elements: (η^6-mesitylene)tin(II) chloride tetrachloroaluminate(III), a coordination polymer. *Heteroat. Chem.* **1990b**, *1*, 161–165.

Schmidbaur, H.; Probst, T.; Steigelmann, O. A triptycene complex of tin(II): $[(C_{20}H_{14})SnCl(AlCl_4)]_2$. *Organometallics* **1991**, *10*, 3176–3179.

Schneider, S.; Dzudza, A.; Raudaschl-Sieber, G.; Marks, T. J. Copper(I) *tert*-butylthiolato clusters as single-source precursors for high-quality chalcocite thin films: precursor chemistry in solution and the solid state. *Chem. Mater.* **2007**, *19*, 2768–3779.

Sheldrick, W. S.; Martin, C. Preparation and crystal-structures of chlorophenylantimonates(III) and bromophenylantimonates(III) $[Ph_2SbX_2]^-$ and $[Ph_2Sb_2X_7]^{3-}$ (X=Cl, Br). *Z. Naturforsch., B: Chem. Sci.* **1992**, *47*, 919–924.

Shevchenko, D. V.; Petrusenko, S. R.; Kokozay, V. N.; Zhigalko, M. V.; Zubatyuk, R. I.; Shishkin, O. V.; Skelton, B. W.; Raithby, P. R. Heterobimetallic M/Zn (M=Cu, Ni) complexes with open-chain N- and N,O-ligands: template synthesis from metal powders and supramolecular crystal structures. *Inorg. Chim. Acta* **2005**, *358*, 3889–3904.

Su, Z.; Sun, K.; Han, Z.; Liu, F.; Lai, Y.; Li, J.; Liu, Y. Fabrication of ternary Cu-Sn-S sulfides by a modified successive ionic layer adsorption and reaction (SILAR) method. *J. Mater. Chem. A* **2012**, *22*, 16346–16352.

Tanaka, T.; Kawasaki, D.; Nishio, M.; Guo, Q.; Ogawa, H. Fabrication of Cu_2ZnSnS_4 thin films by co-evaporation. *Phys. Status Solidi C* **2006**, *3*, 2844–2847.

Temple, D. J.; Kehoe, A. B.; Allen, J. P.; Watson, G. W.; Scanlon, D. O. Geometry, electronic structure, and bonding in $CuMCh_2$(M=Sb, Bi; Ch=S, Se): alternative solar cell absorber materials? *J. Phys. Chem. C* **2012**, *116*, 7334–7340.

Veith, M.; Godicke, B. Huch, V. Darstellung und strukturen von chlorostannaten(II). II. Neue chlorostannate(II) von zweiwertigen kationen. *Z. Anorg. Allg. Chem.* **1989**, *579*, 87.

Wang, W.; Shen, H.; Li, J. Rapid synthesis of hollow CTS nanoparticles using microwave irradiation. *Mater. Lett.* **2013**, *111*, 5–8.

Weininger, M. S.; Rodesiler, P. F.; Amma, E. L. Metal ion-aromatic complexes. 24. Synthesis and crystal structure of chloro(π-aryl) tin(II) tetrachloroaluminate containing the $Sn_2Cl_2^{2+}$ moiety. *Inorg. Chem.* **1979**, *18*, 751–755.

Wells, A F. Structural Inorganic Chemistry; 5th Edition. Clarendon Press: Oxford, 1984, pp.10–24.

Wielandt, J. W.; Kilah, N. L.; Willis, A. C.; Wild, S. B. Self-assembly of square-planar halide complexes of phosphine-stabilised stibenium salts. *Chem. Commun.* **2006**, *42*, 3679–3680.

Willey, G. R.; Daly, L. T.; Meehan, P. R.; Drew, M. G. B. Controlled hydrolysis reactions of the group 15 element-azamacrocyclic complexes MCl_3L (M=As, Sb or Bi; L=1,4,7-trimethyl-1,4,7-triazacyclononane). Formation and crystal structures of $[AsCl_2L][As_2OCl_5]$, $[H_2L]2[Sb_2OCl_6]Cl_2$, [HL]L and $[H_2L]_2[Sb_2Cl_9]$ $Cl{\cdot}MeCN{\cdot}H_2O$. *J. Chem. Soc., Dalton Trans.* **1996**, *26*, 4045–4053.

Wojtas, M.; Jakubas, R. Structure and properties of $[(CH_3)_4P]_3[Sb_2Cl_9]$ and $[(CH_3)_4P]_3[Bi_2Cl_9]$. *J. Phys.: Condens. Matter* **2004**, *16*, 7521.

Yeh, M. Y.; Lee, C. C.; Wuu, D. S. Influences of synthesizing temperatures on the properties of Cu_2ZnSnS_4 prepared by sol-gel spin-coated deposition. *J. Sol-Gel Sci. Technol.* **2009**, *52*, 65–68.

Zang, Y.; Yin, Z.; Wang, G.; Zeng, C.; Dai, A.; Zhou, Z. Crystal structure and magnetic properties of a novel hetero tetranuclear zinc-copper-copper-zinc complex. *Inorg. Chem.* **1990**, *29*, 560–563.$\{(Me_3P)CuCl]_2.ZnCl_2\}_n$